EPFL

Mechanical structuring

- Mechanical properties of glass
- Precision mechanical machining
- Ultrasonic machining
- Abrasive jet machining
- References

Elastic modulus

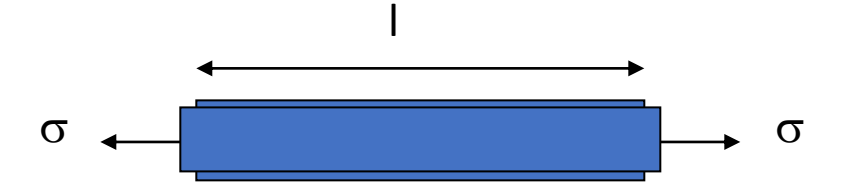


• Elastic modulus : ratio of of the strain, ϵ , resulting from application of a stress σ :

modulus

E: elastic modulus, Young's $\sigma = \frac{E}{1 - \epsilon}$

v : Poissbn's ratio



 $1/1\Delta=3$

- *E* is determined by the atomic bonds and by the structure of the network
- Typical value : 10 100 GPa

2021

Hardness (i)



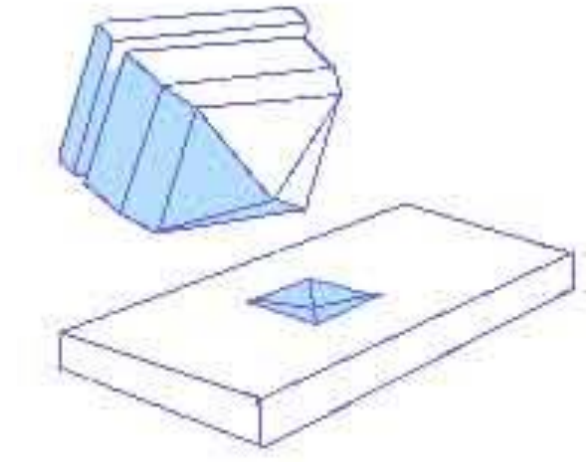
Moh's scale (Friedrich Moh, German mineralogist, 1822):

- 10 Diamond
- 9 Corundum
- 8 Topaz
- 7 Quartz
- 6 Feldspar
- 5 Apatite Glass: 5 7
- 4 Fluorspar
- 3 Calcite
- 2 Gypsum
- 1 Talc

Prof. M.A.M. Gijs, Dr. V.K. Parashar, Swiss Federal Institute of Technology Lausanne (EPFL)

Hardness (ii)





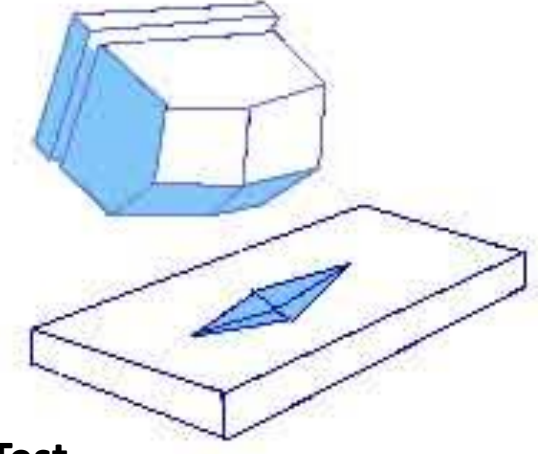
Vickers Test

Opposing indenter faces are set at 136 ° to each other

$$HV = \frac{1.854F[kgf]}{A[mm^2]}$$

Glass: HV ~ 2-8 GPa

Diamond: HV ~ 100 GPa



Knoop Test

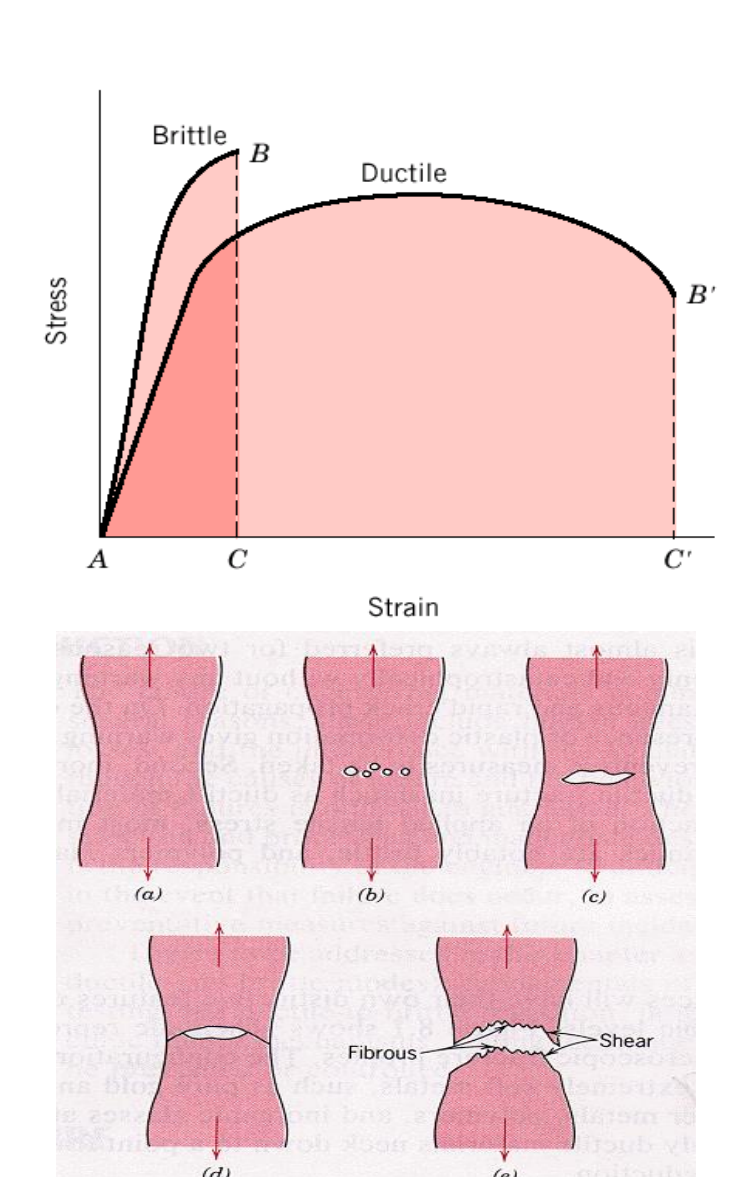
Long side faces are set at a 172 ° 30` to each other. Short side faces are set at a 130 ° to each other

$$HK = \frac{14.2F[kgf]}{A[mm^2]}$$

Toughness (metals)

EPFL

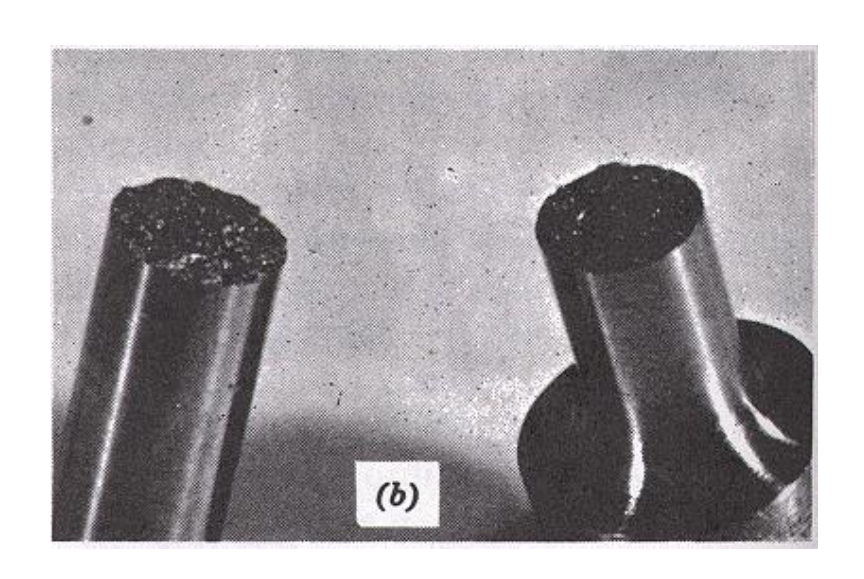
- Toughness: ability to absorb energy in the plastic range up to fracture
- Proportional to area under the strain-stress curve up to fracture
- Units: energy per unit volume, e.g. J/m³



Fracture (brittle materials)



- Two steps in the process of fracture:
 - Crack initiation
 - Propagation
- Exhibits little or no plastic deformation and low energy absorption before failure
- Crack propagation spontaneous and rapid
- Occurs perpendicular to the direction of applied stress, forming an almost flat fracture surface
- Deemed unstable as it will continue to grow without the aid of additional stresses



Griffith theory of brittle fracture

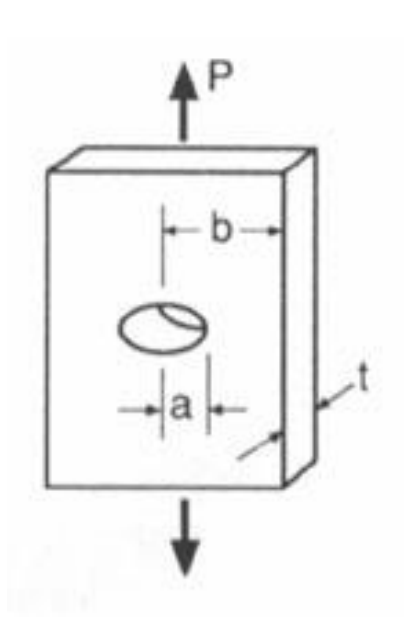
EPFL

 The critical stress required for crack propagation in a brittle material is given by:

$$\sigma_c = \left(\frac{2E\gamma_s}{\pi a}\right)^{1/2}$$

E = modulus of elasticity $\gamma_s = \text{specific surface energy}$ a = half the length of an internal crack

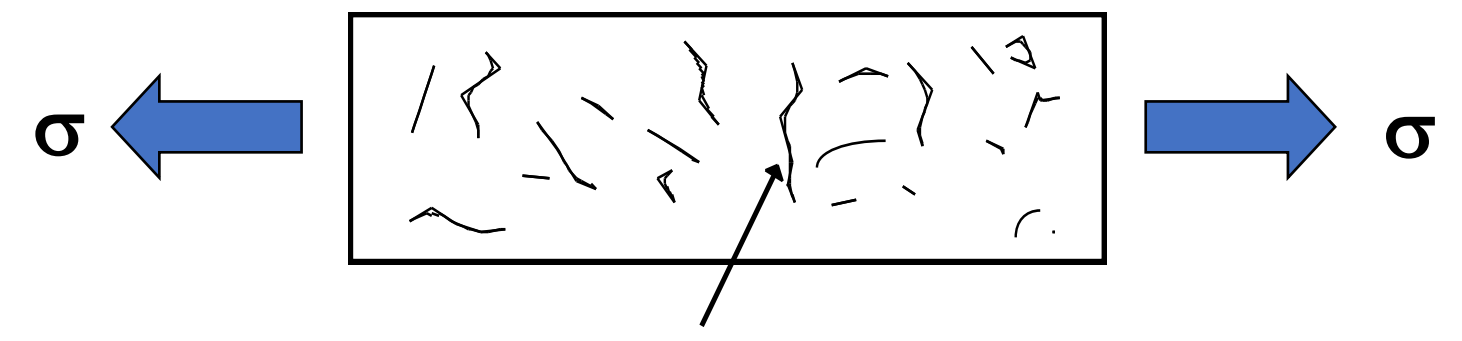
 Applies only in cases where there is no plastic deformation present.



Defect controlled strength



• It is not possible to define the strength of a glass, because the strength is determined by the largest defect (crack) present in a given sample



• Thus strength is determined by a combination of a materials parameter (toughness) and a variable (crack size)

Fracture Toughness



- Stresses near the crack tip of a material can also be characterized by the stress intensity factor, K,
- A critical value of K exists, similar to the value σ_c , known as fracture toughness given by:

$$K_c = Y\sigma\sqrt{\pi a}$$

- Y is a dimensionless parameter that depends on both the specimen and crack geometries.
- Carries the unusual units of MPa m^{1/2}

Defects



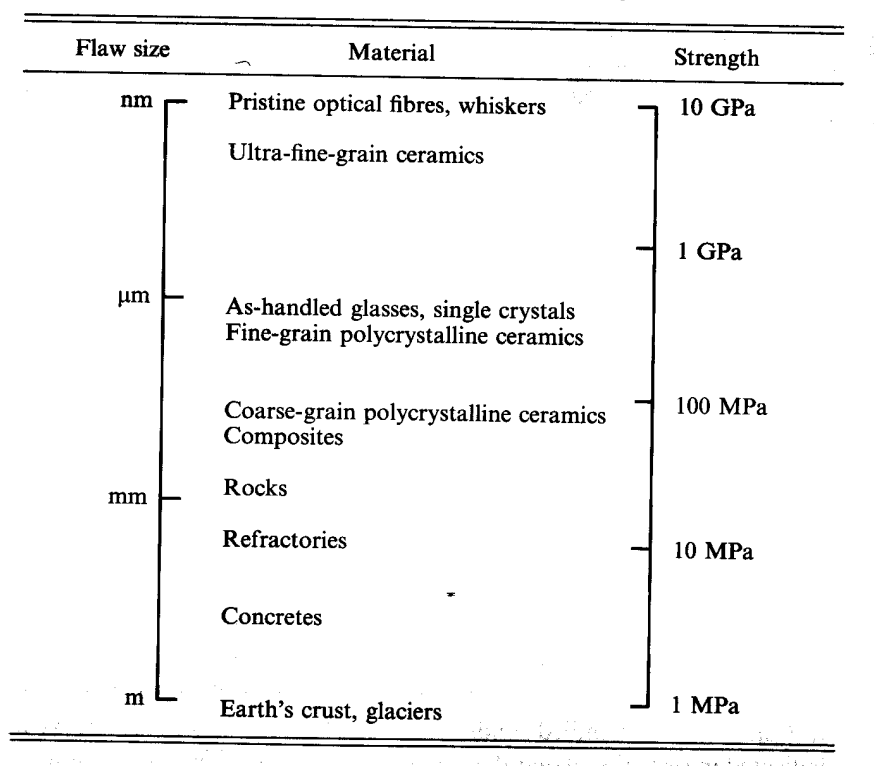
- Fracture toughness is not a variable, so the variation in strength must come from a variation in the size of the biggest defect
- Note that it is the biggest defect which is significant, lots of small defects are stressed but do not reach their critical stress for propagation
- Sources of defects
 - Flaws from imperfect sintering
 - Impact, contact and abrasion damage

Size of defects



- Most brittle materials have fracture toughness in the range 1 - 5 MNm^{-3/2}
- Thus we can estimate likely critical defect size from the measured fracture stress
- Typical engineering ceramics have critical defects about 1 -10 μm

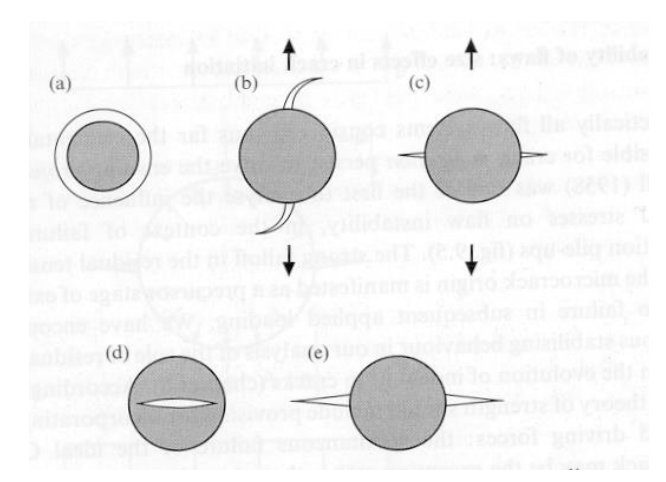
Table 9.1. Typical 'Griffith' flaw sizes and strengths of brittle materials.

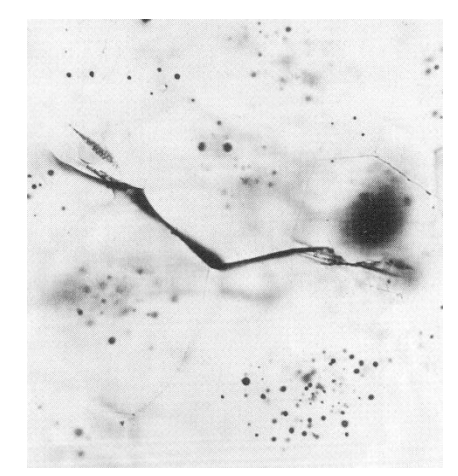


Defects from thermal expansion mismatch

EPFL

- Inorganic impurities (e.g. dust or contaminants) are retained as inclusions
- If they have a different expansion coefficient they will generate internal stress on cooling from sintering temperature
- Also possible if a monolithic material has anisotropic thermal expansion. In which case polycrystals will contain stresses
- Stresses can lead to fracture





Blunt contact defects (i)



- Distinguish between blunt and sharp contact
- Blunt contacts are approximated to the contact of a sphere
- Contact problem solved by Hertz - Hertzian contact
- Deformation is all *elastic* and the contact region is a circle of radius a

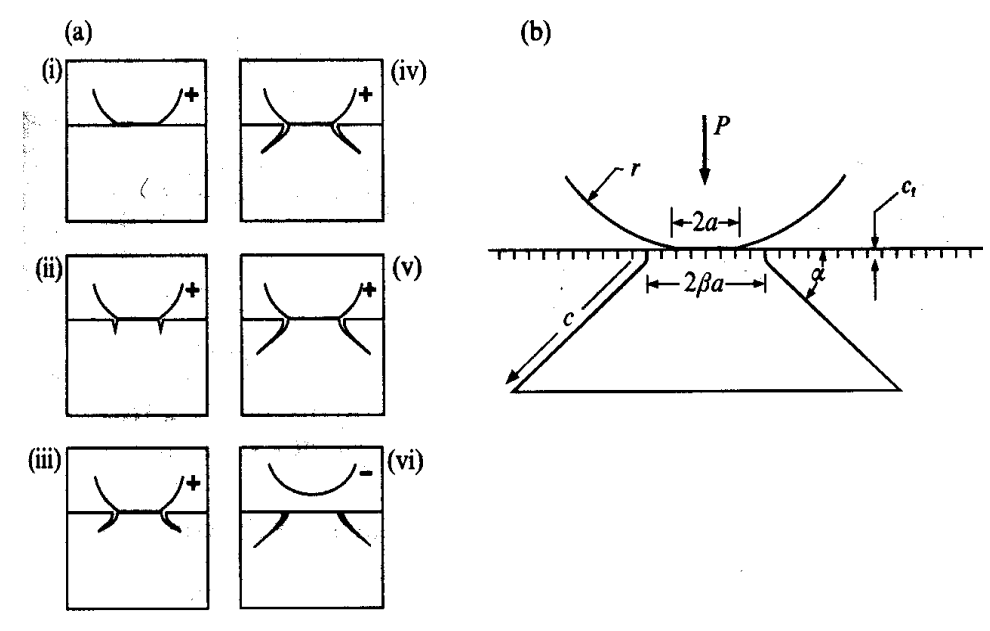
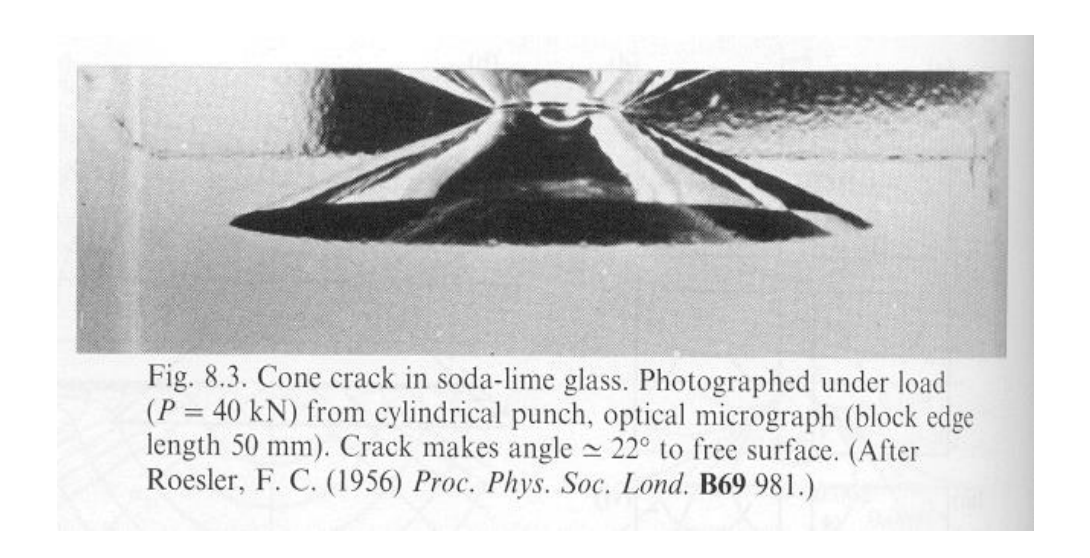


Fig. 8.2. Hertzian cone crack system. (a) Evolution of cone during complete loading (+) and unloading (-) cycle. (b) Geometrical parameters.

Blunt contact defects (ii)



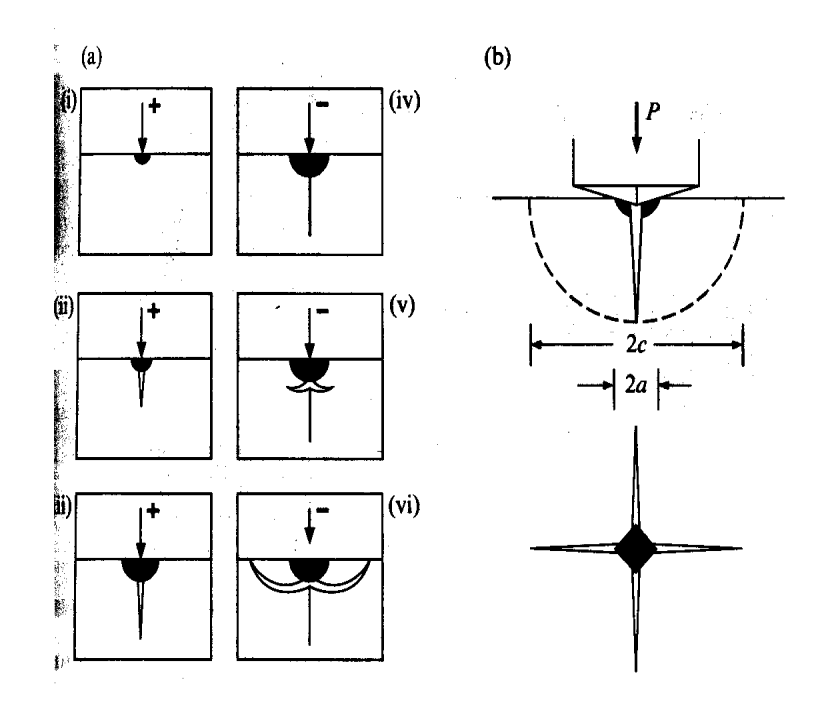
- For a 1 μ m ball on glass a force of 2.5 mN will generate a contact pressure of 10 GPa
- Stress beneath contact is compressive, but at surface just outside the contact it is tensile of similar magnitude
- Contact stresses can nucleate cracks. These propagate in a ring around the contact and then travel into the material as a characteristic cone crack



Sharp contact defects



- Indentation by a point contact leads to a singularity in the stress field beneath the contact
- Plastic flow occurs just below the contact point.
- At some critical load defects in the material cause radial cracks to form on tensile median planes These cracks propagate downwards on increased load
- On unloading the median cracks close up below the surface but open at the surface as plastic deformation leads to a residual tension



• Finally just before unloading a new set of *lateral cracks* parallel to the surface may be nucleated in the residual tensile field

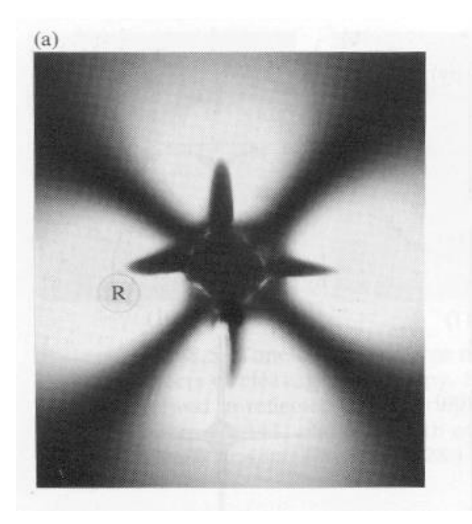
Sharp contact

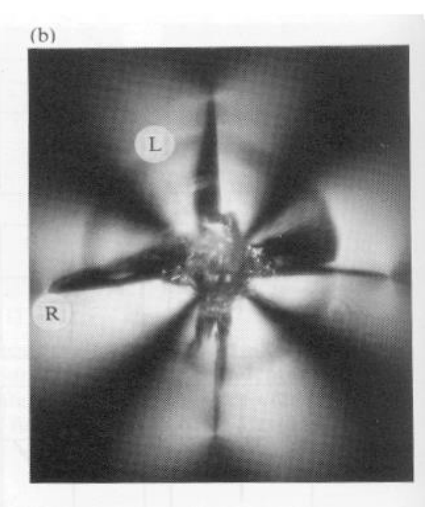
EPFL

- Radial/median crack system first under load from a pyramid diamond indenter (Vickers)
- Then unload radial cracks open further because of residual stress
- Growth of radial crack

 exposed by fracture

 through the indent



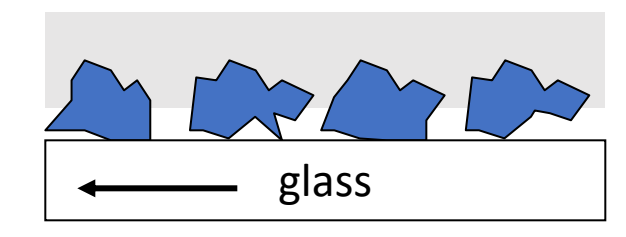


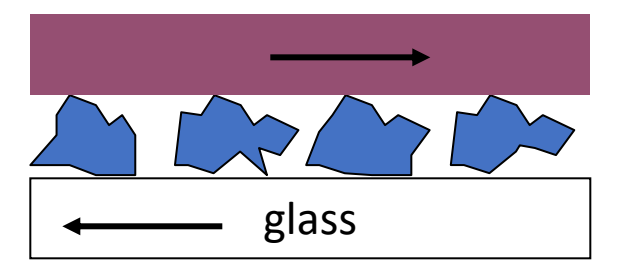
Abrasion and erosion

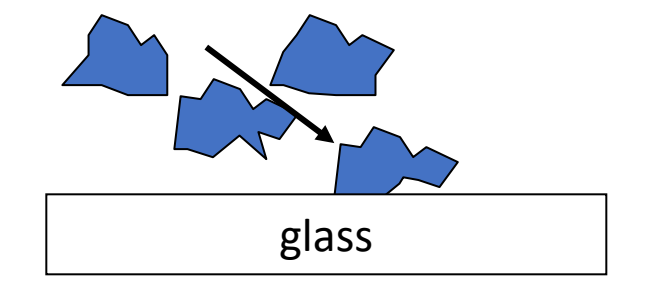


- Defects and cracks are at the basis of glass micropatterning
- Grinding or two-body abrasion

 abrasive particles are
 embedded in adhesive backing
 grinding, sawing, precision
 machining
- Three-body abrasion: loose particles in a carrier fluid are contained between workpiece and backing plate → ultrasonic machining
- Solid particle erosion : particles in a gas stream strike the glass surface → powder blasting



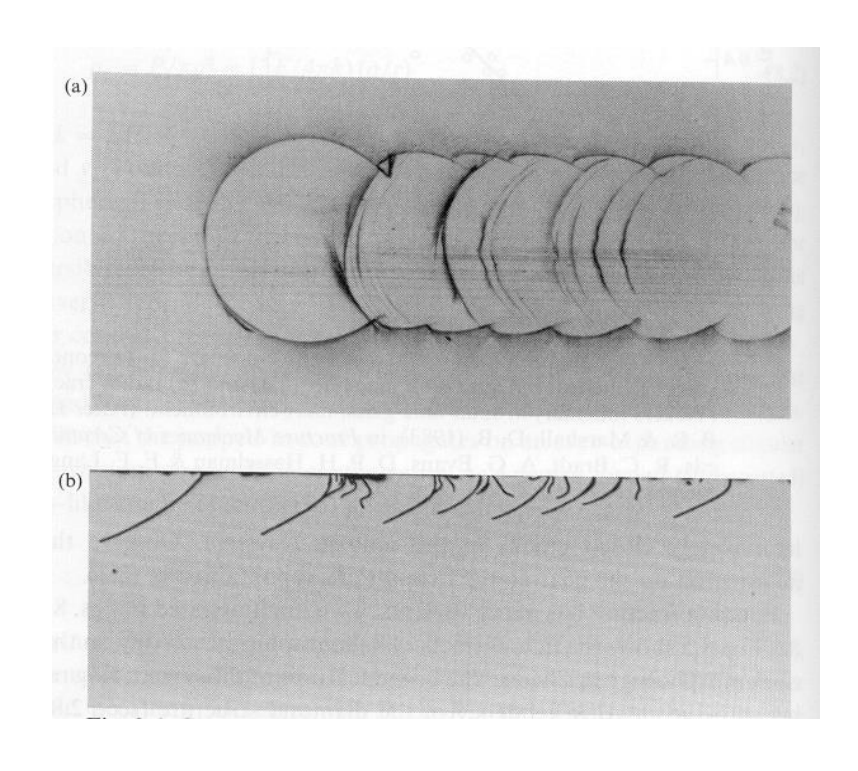


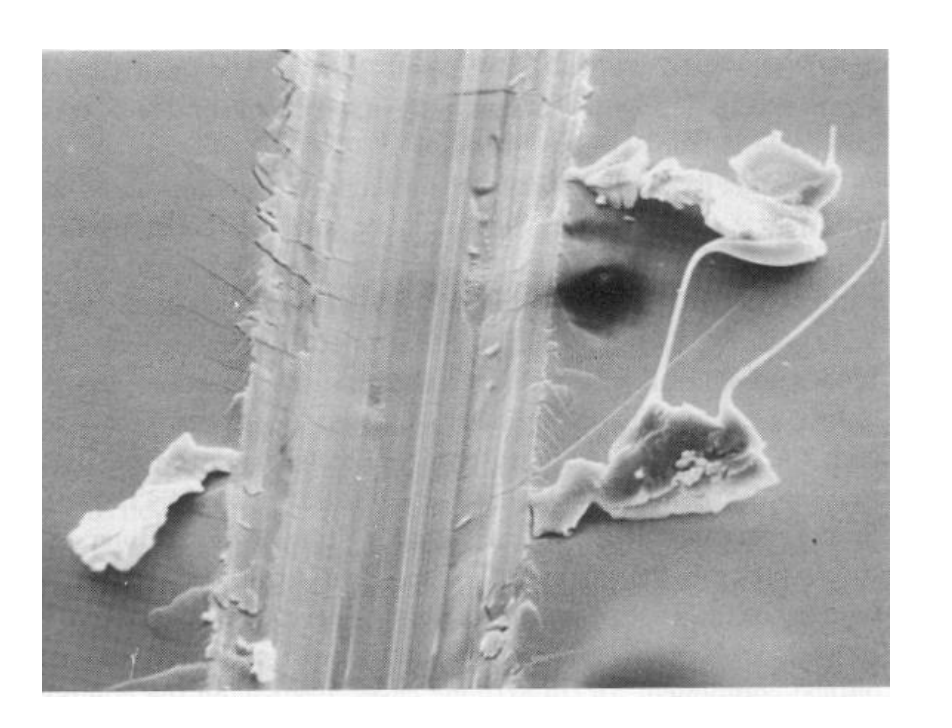


Two-body abrasion



- Repeated cone cracks from a blunt slider
- Sharp slider causes local plastic flow; radial and median crack families will be present

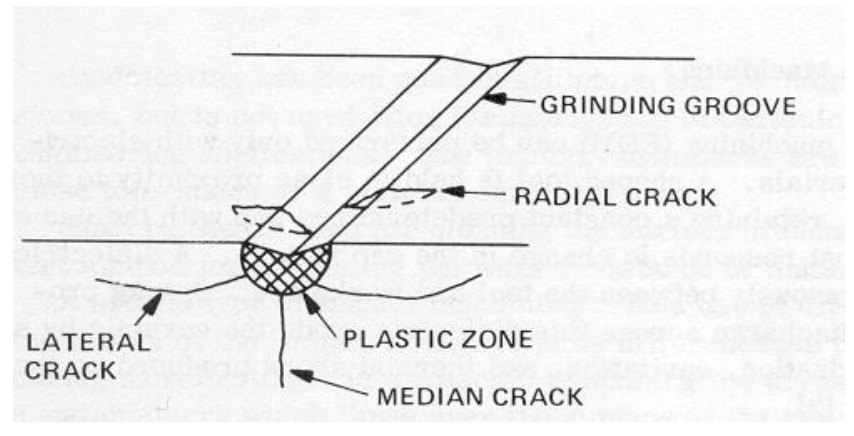


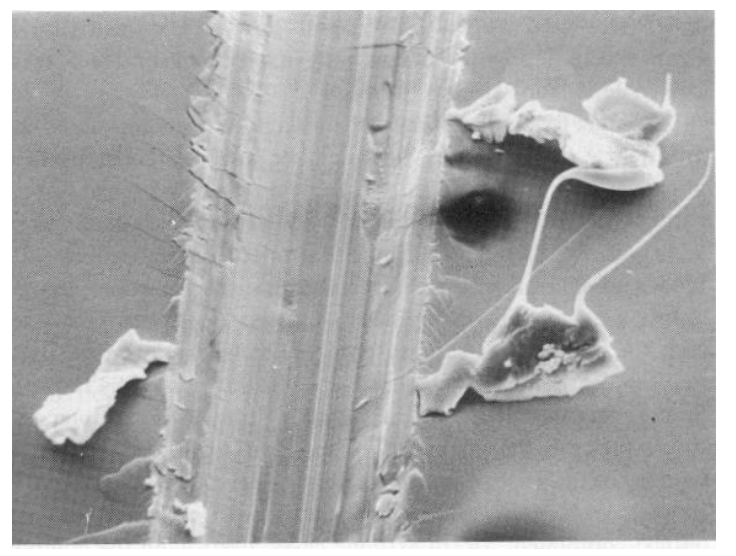


Precision glass machining



- Machining normally in the form of grinding
- Multiple impact and scratching from diamond particles embedded in a wheel
- These leave a large median crack – major strength reduction
- Also radial and lateral cracks –lateral cracks remove material by spalling





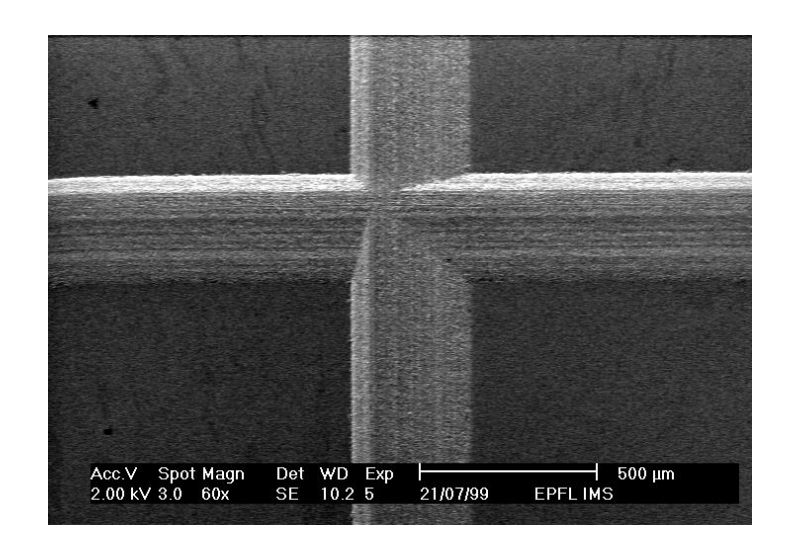
Machining process

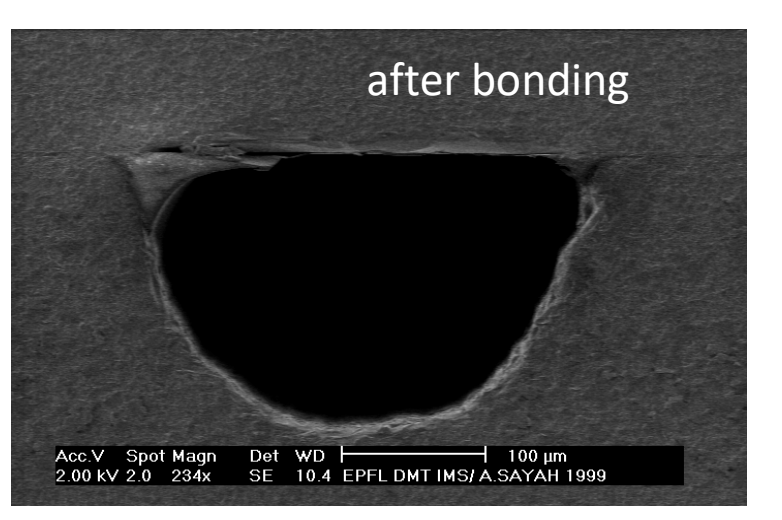


- Try and make glass object as "near-net-shape"
- Diamond machining first uses large grit size for efficient material removal
- This introduces large median cracks (scales with particle size)
- Repeated grinding at 90° to the previous grinding direction with finer grit size
- Objective is to completely machine off median defect and replace with a smaller scale version
- Continue with repeated reductions in diamond size until desired finish is achieved

Machining (sawing)

- microchannels
 Minimum saw blade thickness and channel width is $30 \mu m$.
- Technique has the advantage to be simple and fast
- No mask is necessary and there is no need of clean room environment.
- Only simple straight channels possible



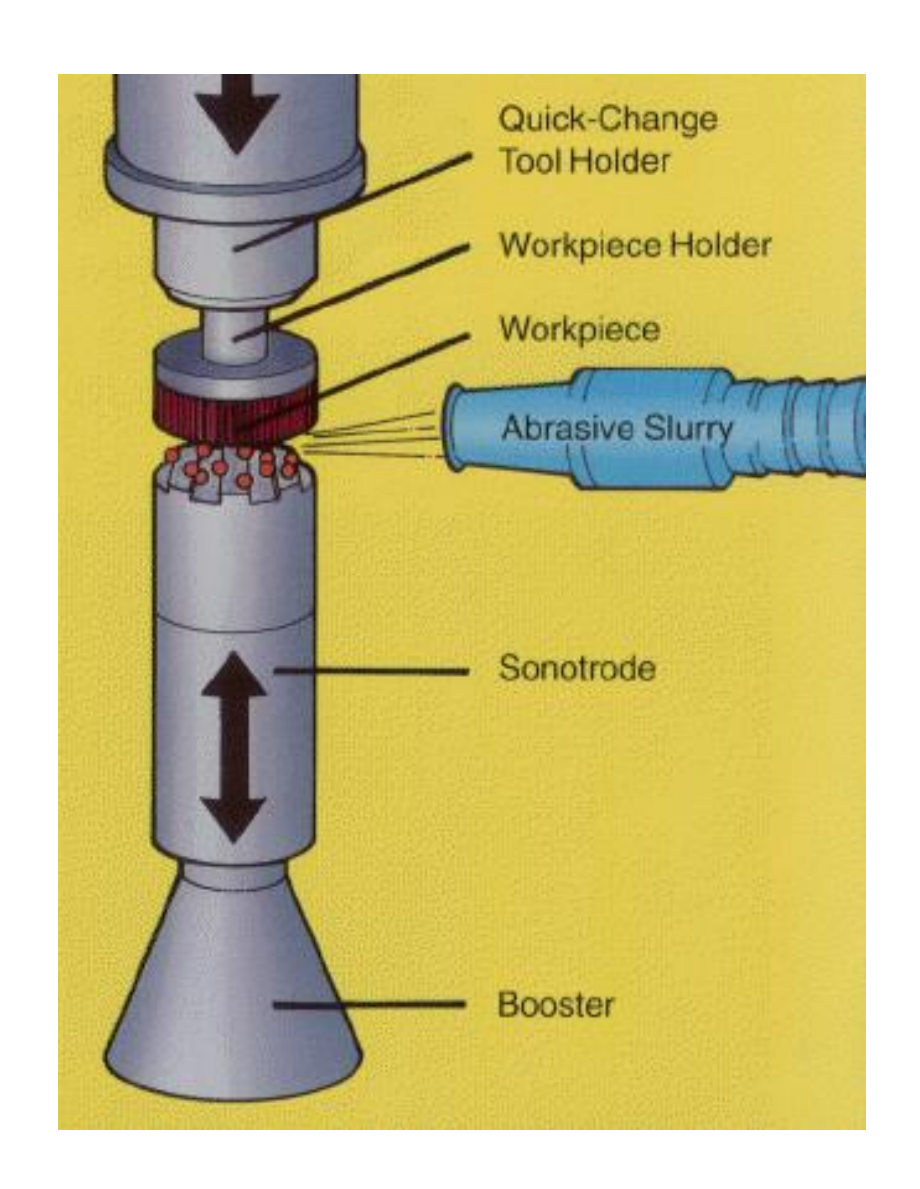




Principle of ultrasonic machining (i)

- Material is removed by micro-chipping or erosion with abrasive particles.
- The tool, made of softer material than that of the workpiece, is oscillated by the Sonotrode at a frequency of about 20 kHz
- It forces the abrasive grits, in the gap between the tool and the workpiece, to impact on the work surface, thereby machining the work surface.





Principle of ultrasonic machining (ii)

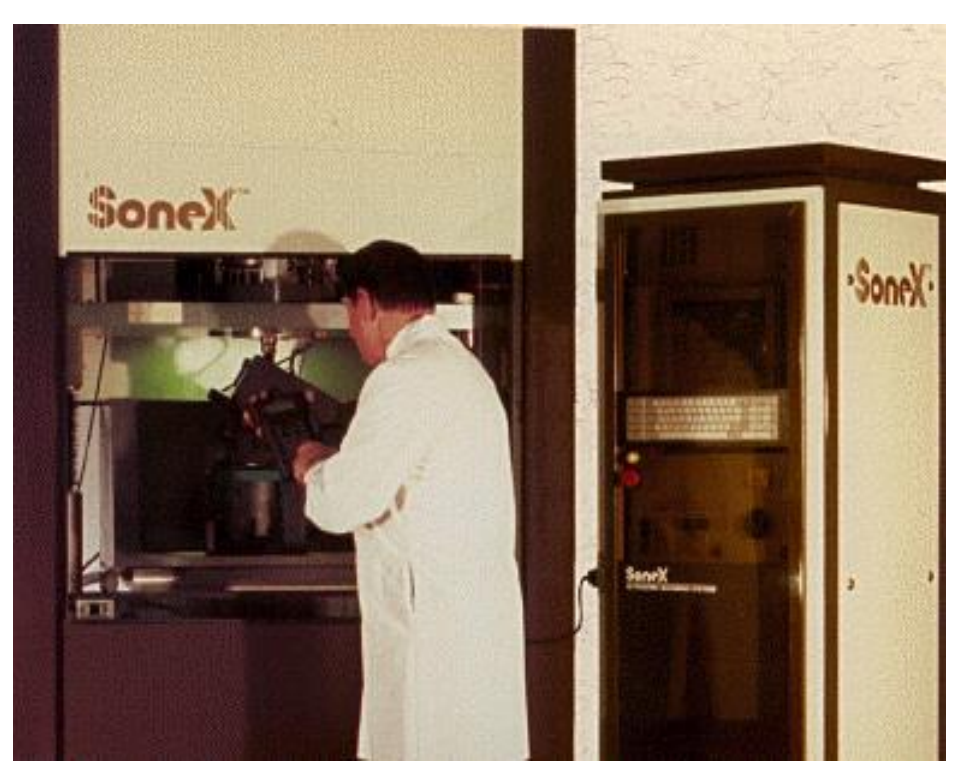


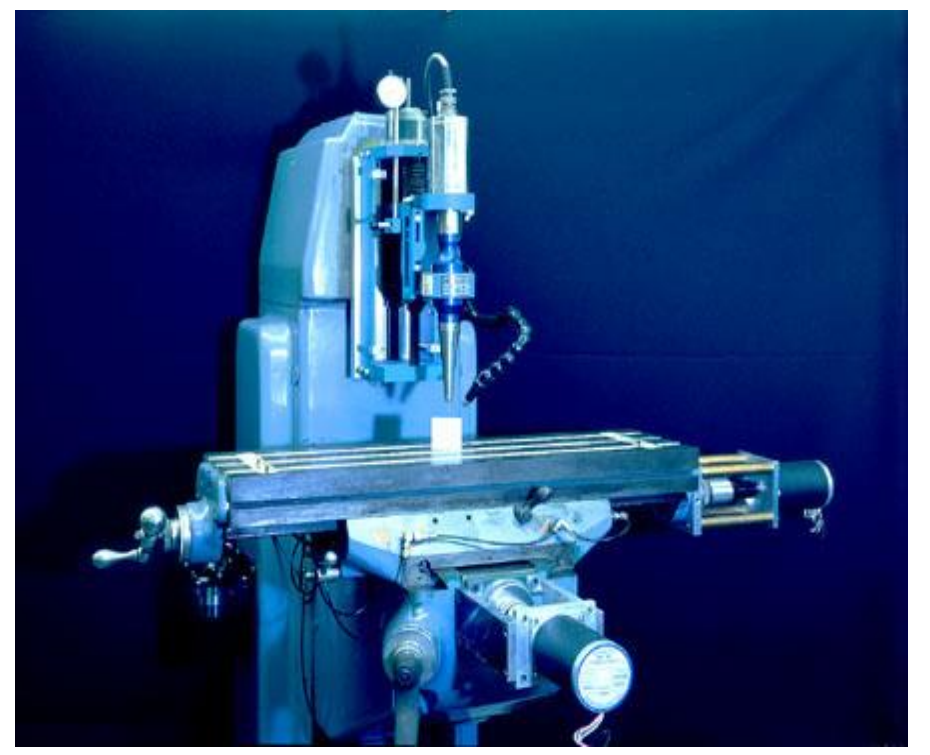
- During one strike, the tool moves down from its most upper remote position with a starting speed at zero.
 It speeds up in this period and finally reaches the maximum at the mean position.
- When the grit size is close to the mean position, the tool hits the grit with its full speed.
- The smaller the grit size, the lesser the momentum it receives from the tool. Therefore, there is an effective speed zone for the tool and, correspondingly there is an effective size range for the grits.

Prof. M.A.M. Gijs, Dr. V.K. Parashar, Swiss Federal Institute of Technology Lausanne (EPFL)

CNC Ultrasonic machines







Sonotrode



- Ultrasonic waves are sound waves of frequency higher than 20 000 Hz
- Ultrasonic waves can be generated using the magnetostrictive effect to convert magnetic energy into ultrasonic energy. This is accomplished by applying a strong alternating magnetic field to certain metals, alloys and ferrites.
- Piezoelectric transducers employ the inverse piezoelectric effect using natural or synthetic single crystals (such as quartz) or ceramics (such as barium titanate) which have strong piezoelectric behavior.

Abrasive slurry



- The abrasive slurry contains fine abrasive grains. The grains are usually boron carbide, aluminum oxide, or silicon carbide ranging in grain size from 100 μ m (grit/sieve size 100) for roughing to 5 μ m (grit/sieve size 1000) for finishing.
- It is used to microchip or erode the work piece surface and it is also used to carry debris away from the cutting area.

Machinable materials



- As the ratio of hardness of workpiece and tool increases, metal removal rate decreases
- Hard materials like stainless steel, glass, ceramics, carbide, quartz and semi-conductors are machined by this process.
- Brittle materials can be well machined
- Material removal rate= 5.9 f (s/H) R ^{0.5} y ^{0.5}

where

f = frequency of oscillations, Hz

H = surface fracture strength, BHN

s = static stress in tool, kg/mm2

R = mean radius of grit, mm

y = amplitude of vibration, mm

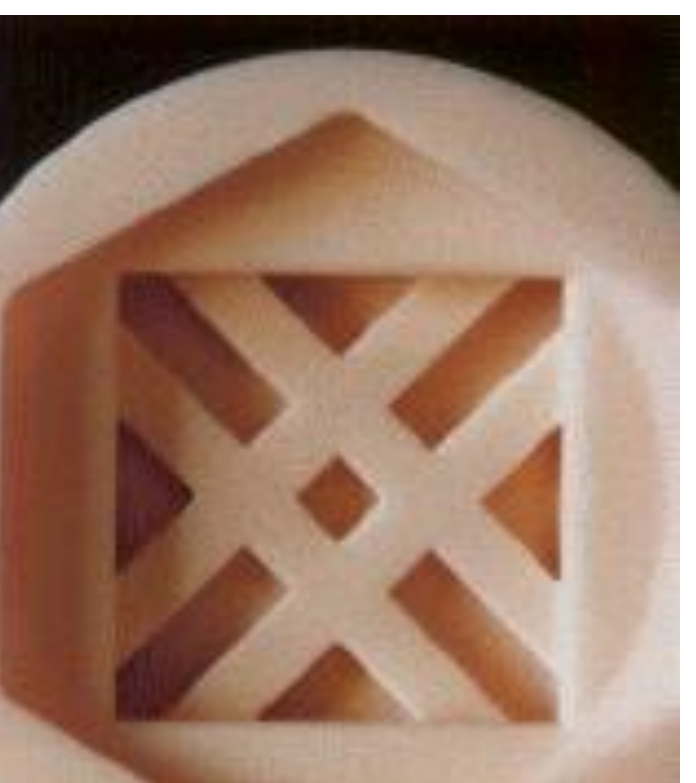
021

Prof. M.A.M. Gijs, Dr. V.K. Parashar, Swiss Federal Institute of Technology Lausanne (EPFL)

Machining of hard plastics



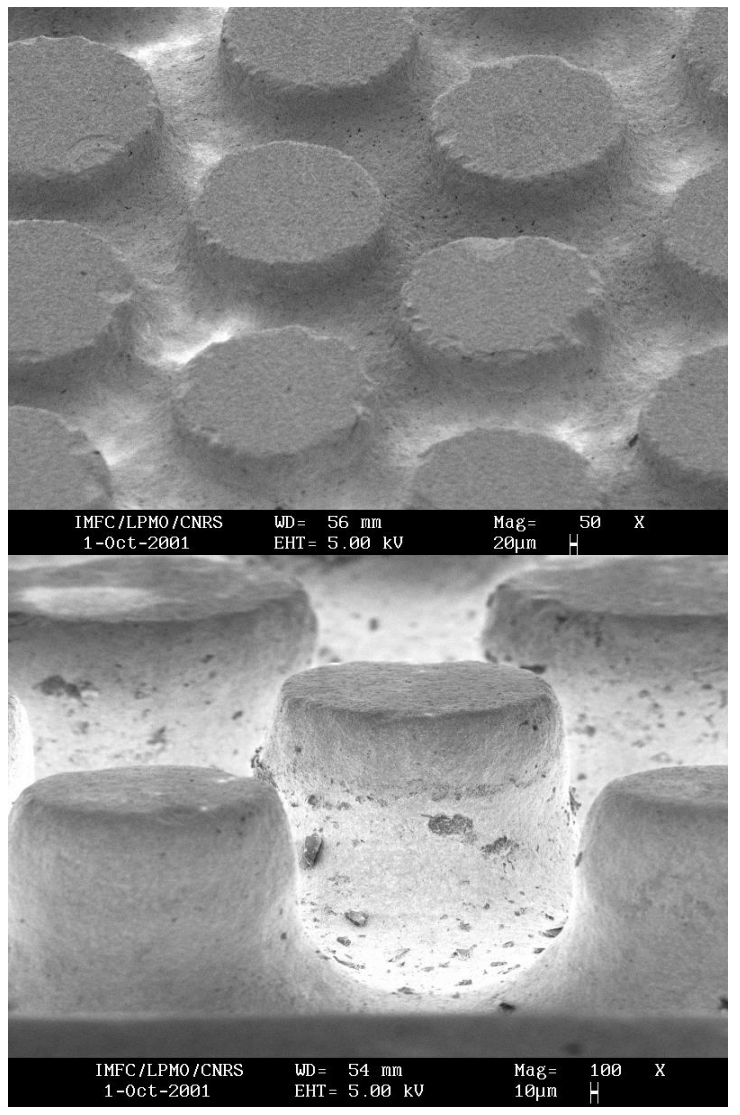




EPFL

Micromachining of PZT pillars for ultrasound transducers (Univ. Franche-Comté, Besançon)





Advantages of USM



- Machining of any materials, regardless of their conductivity
- USM applies to machining of semi-conductors, such as silicon, germanium etc.
- USM is suitable to precise machining of brittle materials
- USM does not produce electrically, thermally, chemically modified surfaces, because action is not electric, thermal or chemical
- Can drill circular or non-circular holes in very hard materials
- Less stress because of non-thermal characteristics

Disadvantages of USM

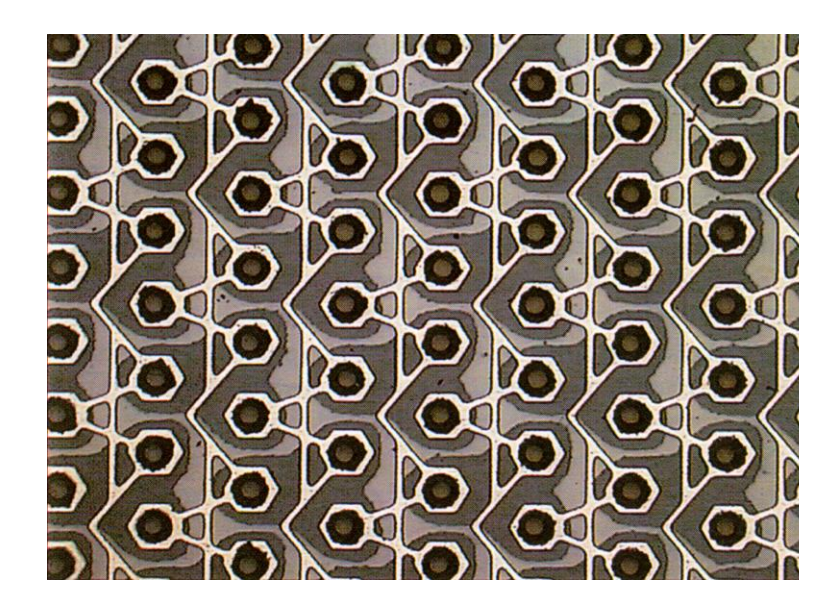


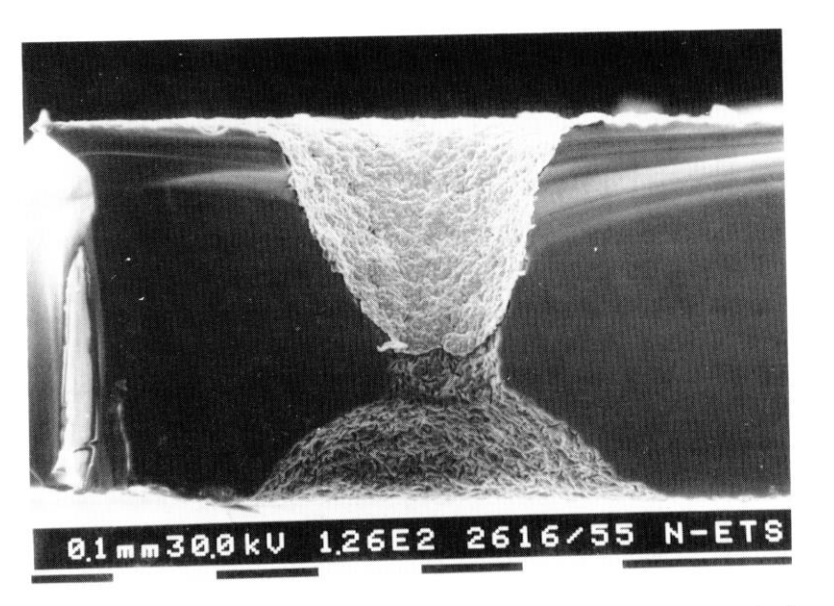
- USM has low material removal rate
- Tool wear fast in USM.
- Machining area and depth is restraint in USM.
- Some numbers
 - Under ideal conditions, penetration rates of 5 mm/min can be obtained.
 - Power units give usually 500-1000 watt output.
 - Specific material removal rate of brittle materials is 0.018 mm³/Joule.
 - Normal hole tolerances are 0.007 mm and surface finish can be 0.02 $0.7 \mu m$.

Micro-powder blasting



Powder blasting developed to high level microfabrication technique for flat panel display applications



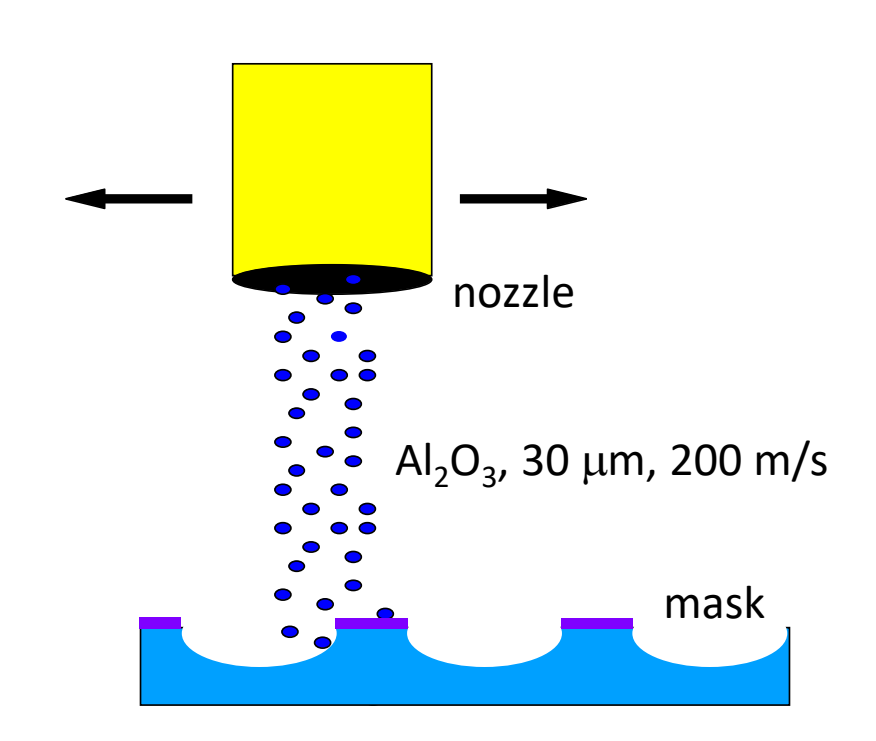


(Philips Research)

Prof. M.A.M. Gijs, Dr. V.K. Parashar, Swiss Federal Institute of Technology Lausanne (EPFL)

Powder blasting: schematic



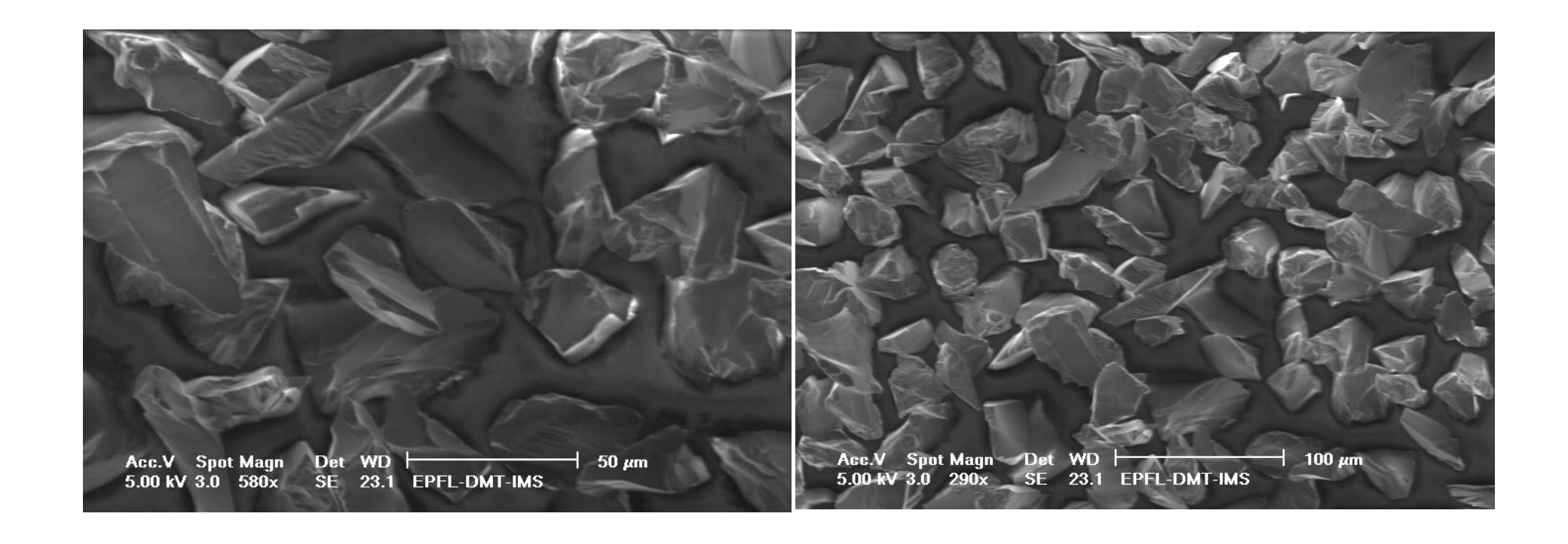


mask:

- steel contact
- soft polymer

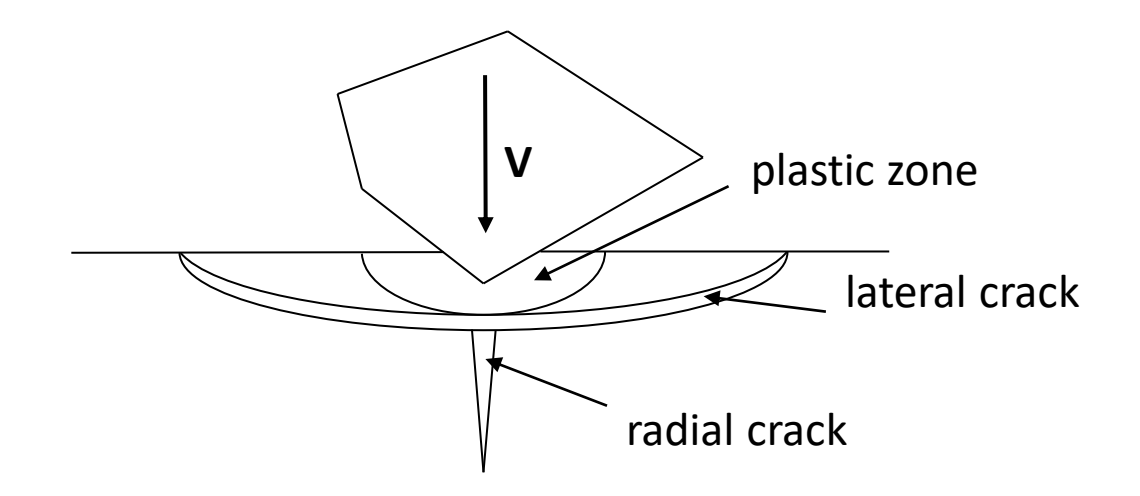
EPFL

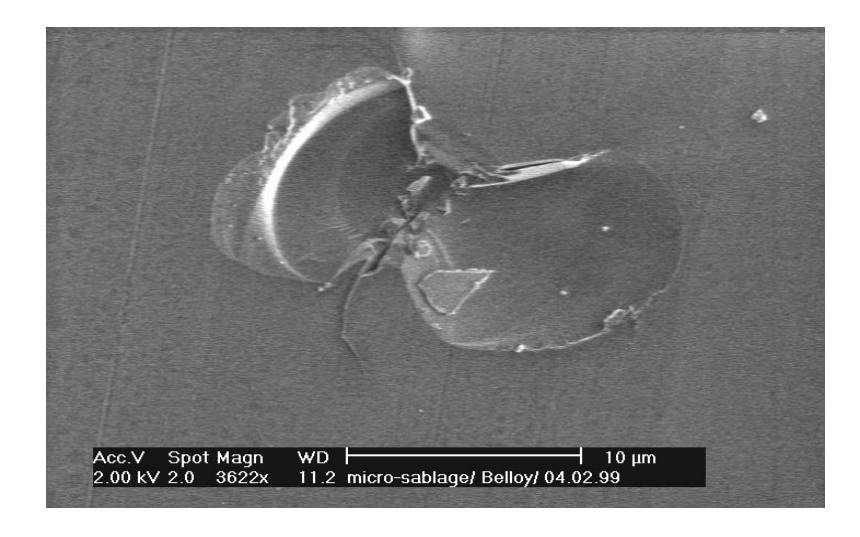
Al₂O₃ powder



Basic mechanism

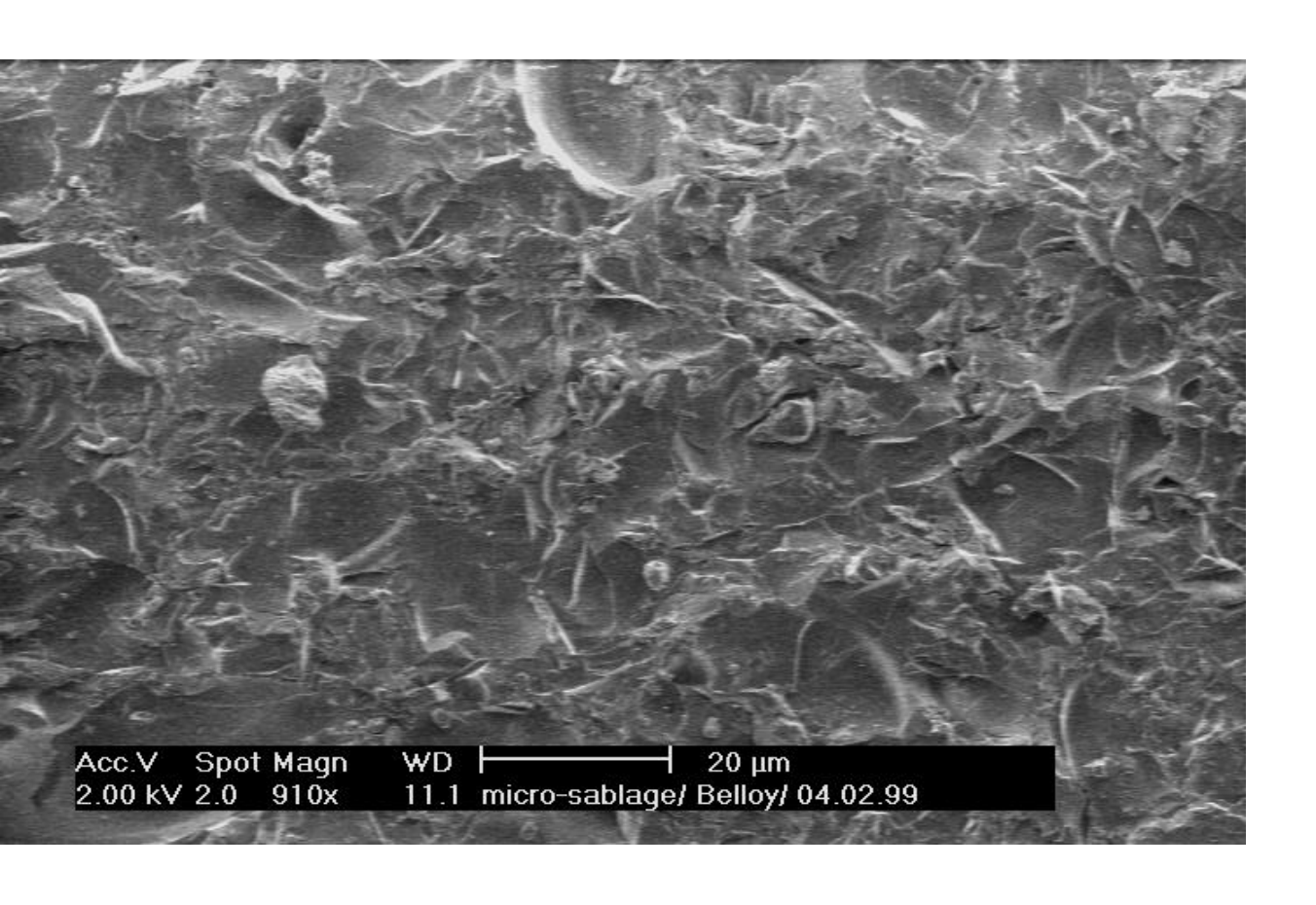






Surface roughness : $0.1-5~\mu m$

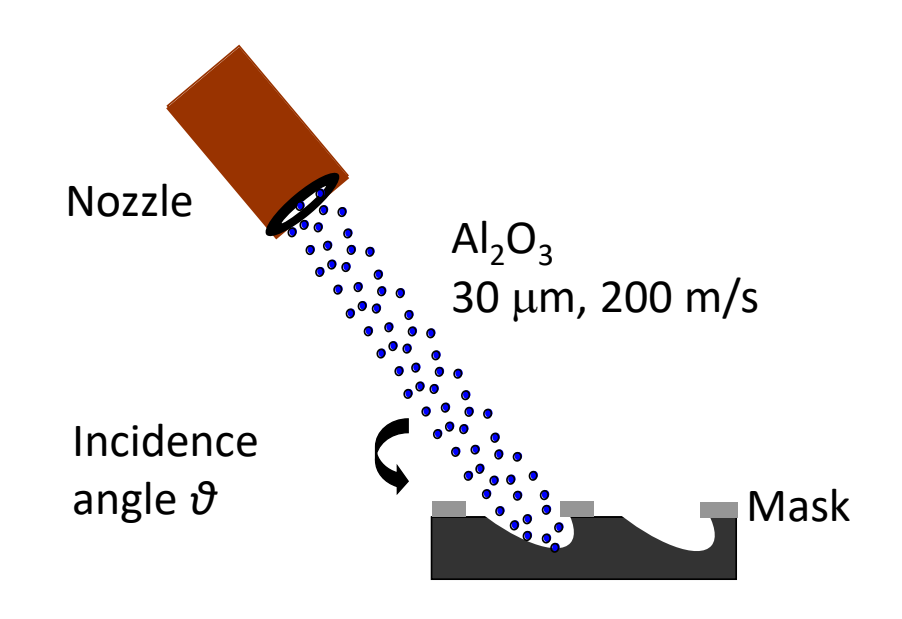




Prof. M.A.M. Gijs, Dr. V.K. Parashar, Swiss Federal Institute of Technology Lausanne (EPFL)

Powder blasting set-up EPFL







Normal vs oblique erosion

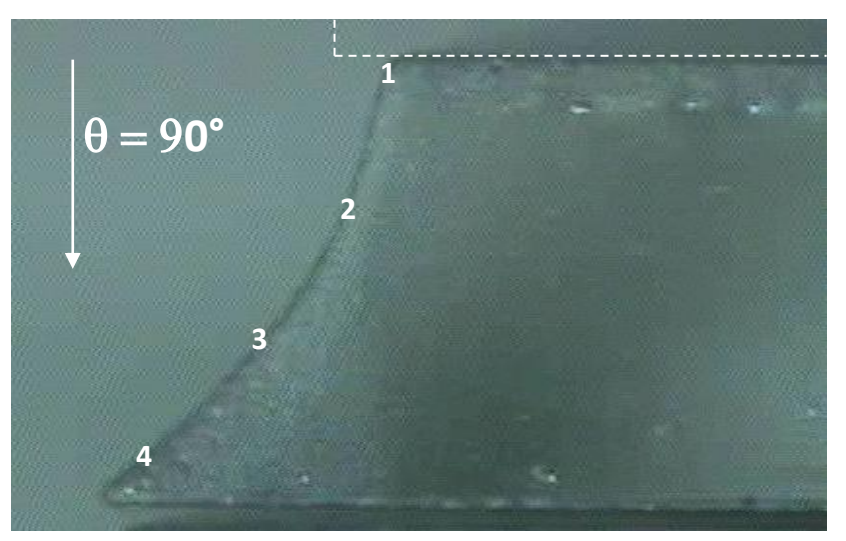


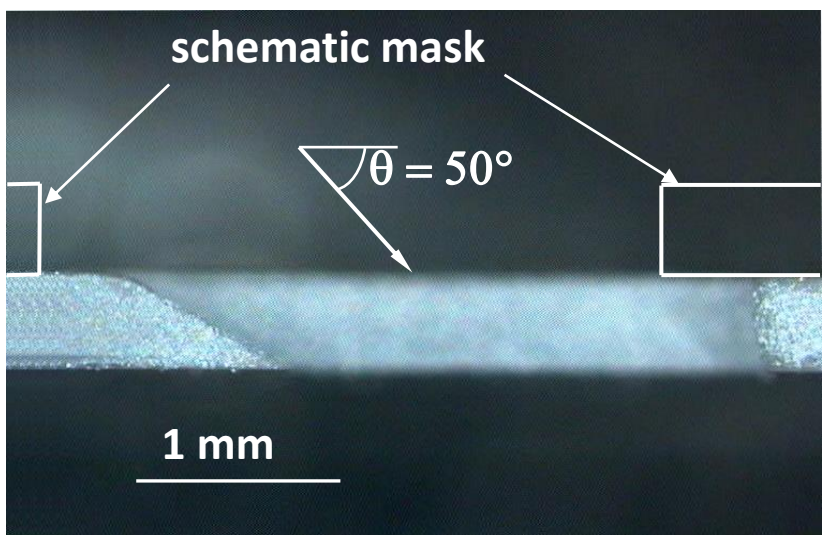
'Natural' profile at normal incidence:

finite size particle effects + normal momentum effect

Oblique profile:

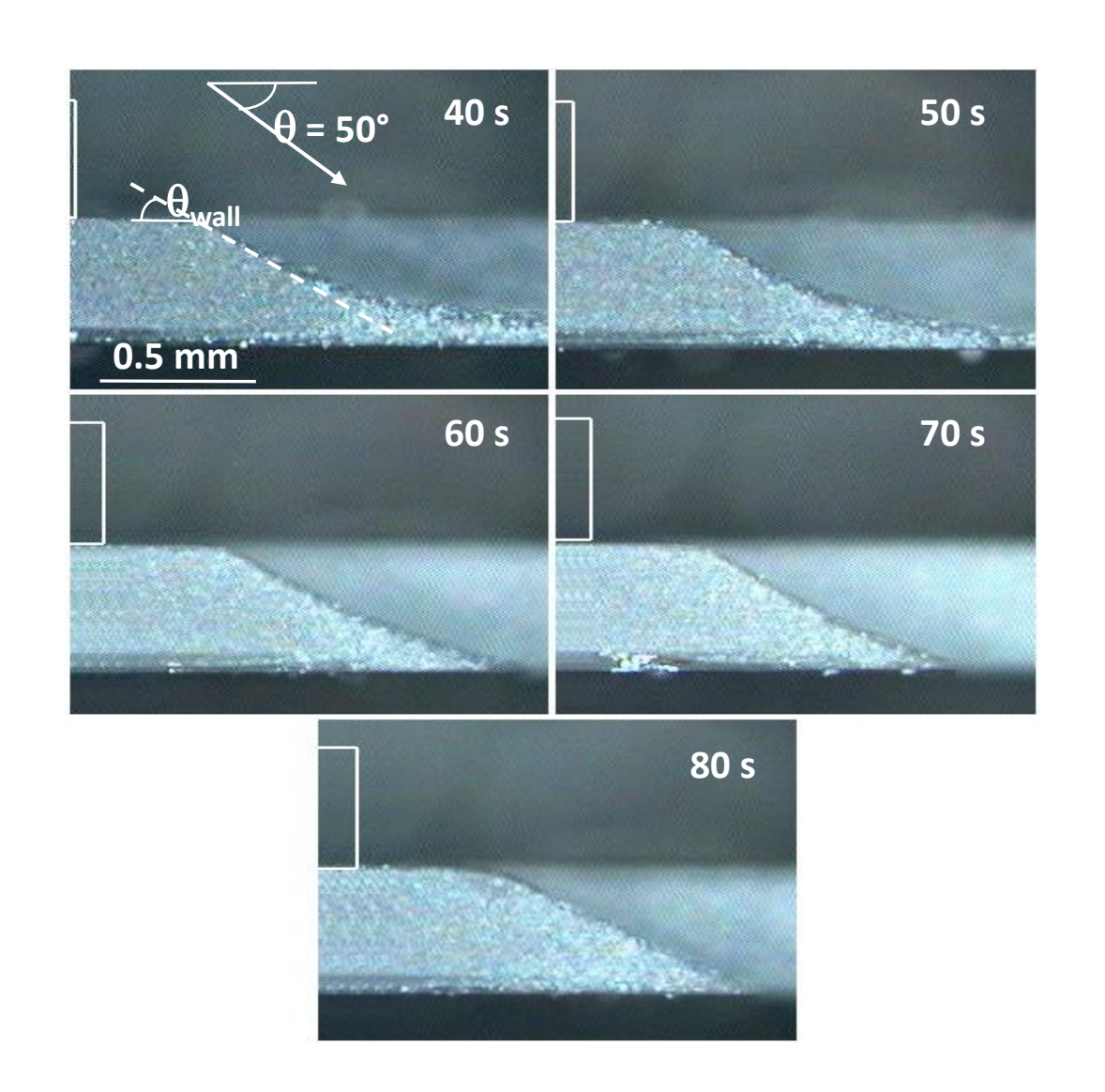
left slope → primary particles right slope → primary + secondary particles





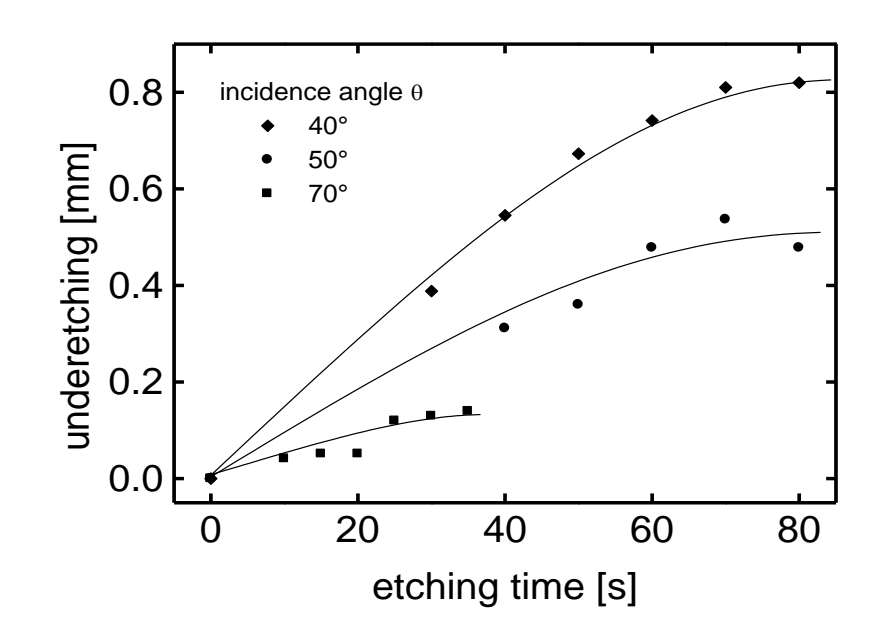
Left wall angle: time evolution

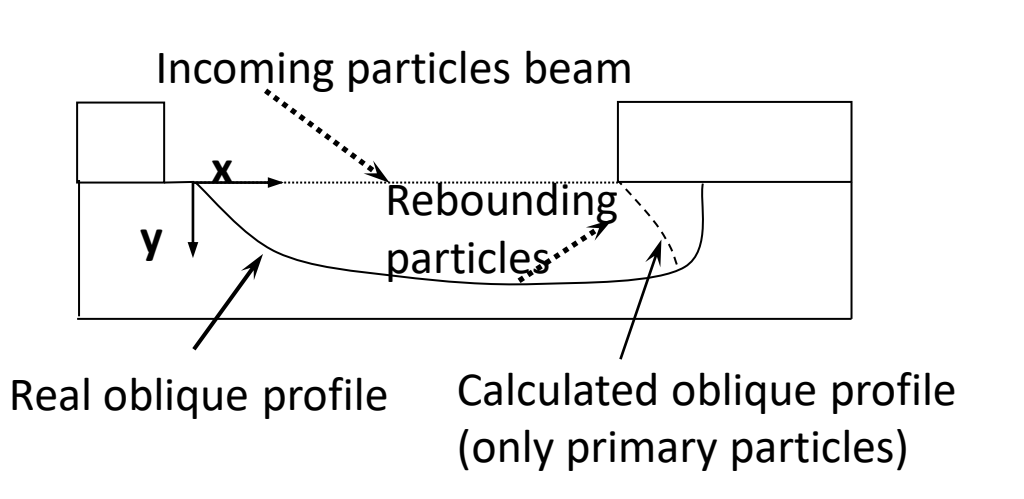




Right-hand slope: underetching







Double-disk system used to determine the particle velocity





Particle speed v:

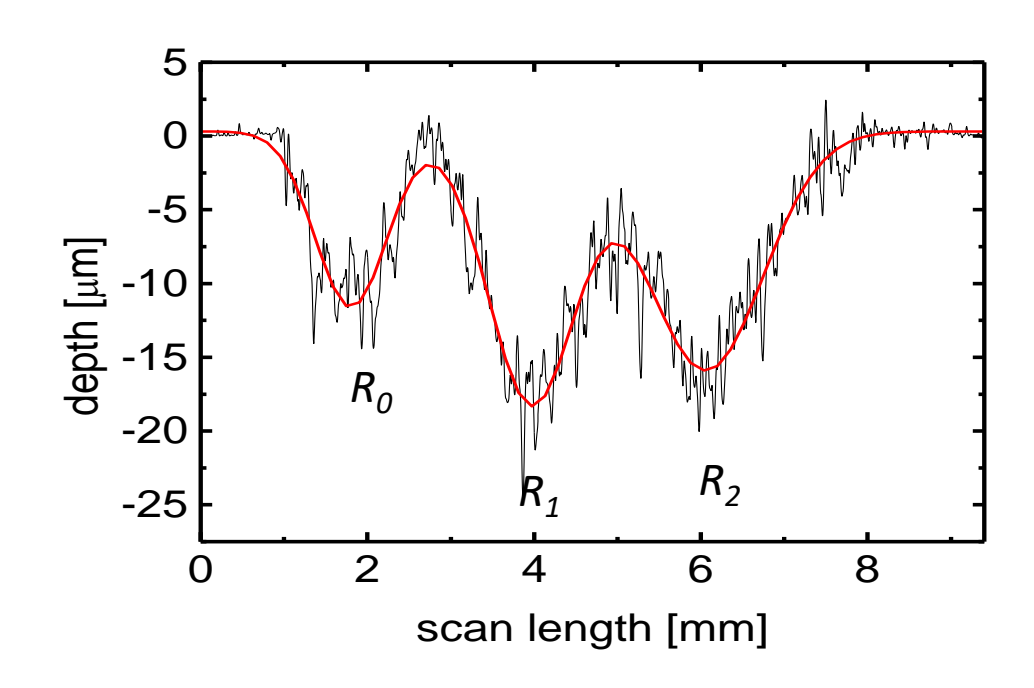
R: rotation speed (rpm)

I: distance between spots

$$v = \frac{2\pi reR}{60l}$$

Erosion profiles

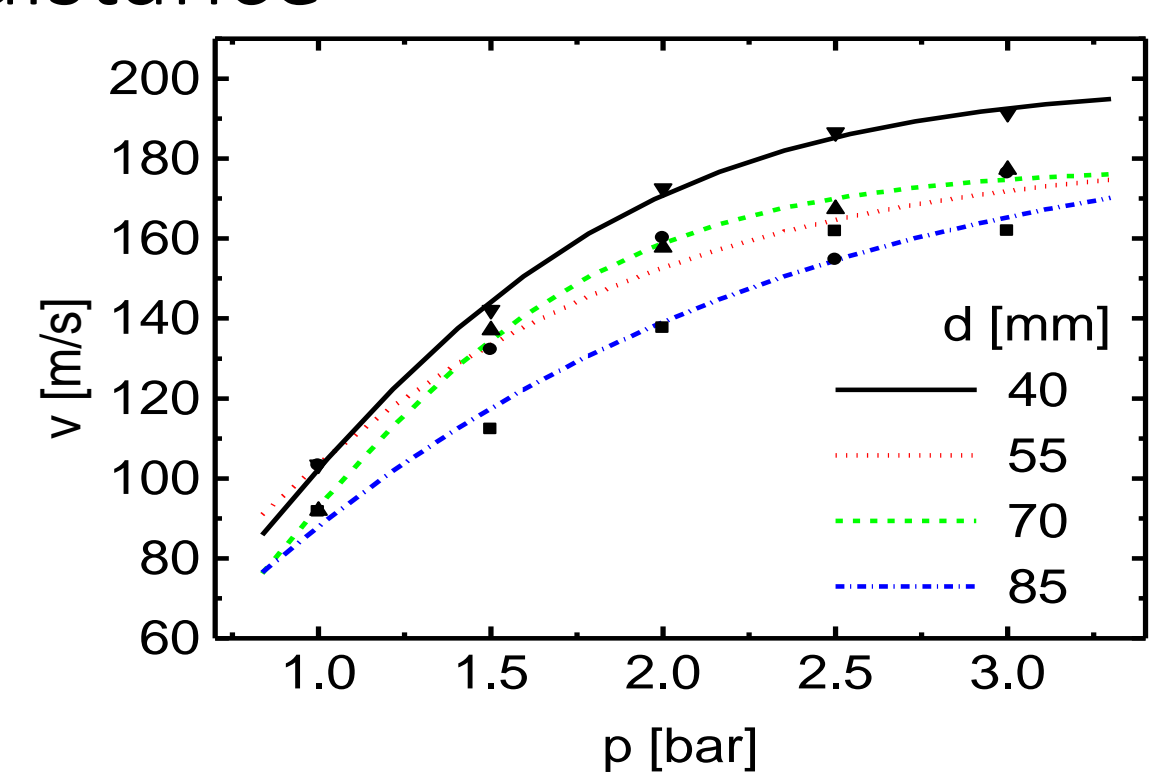




$$R_0$$
 = 0 rpm, R_1 = 6600 rpm, R_2 = 13200 rpm

$$v = 191 \text{ m/s}$$
 for $p = 0.3 \text{ MPa}$ and $d = 4 \text{ cm}$

Particle velocity as a function of pressure and nozzle-target distance





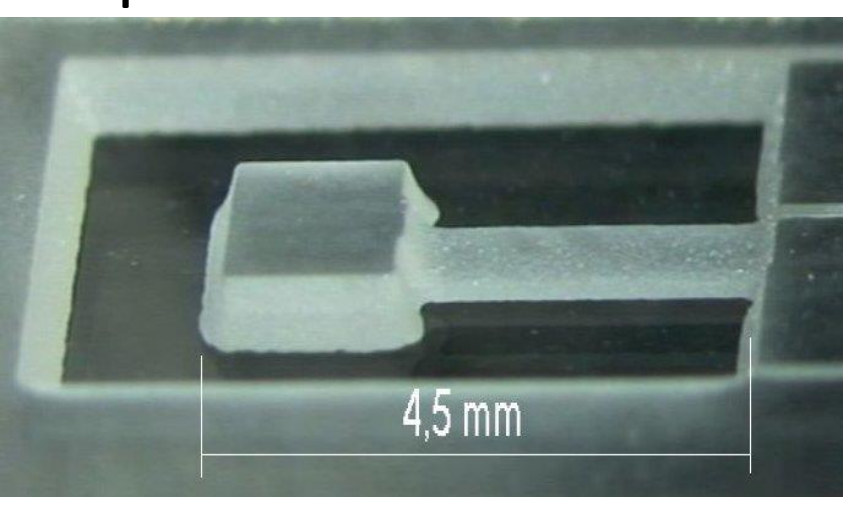
Applications of micro-powder blasting

- Accelerometers
- Cell culture devices
- Fluidic chips for electrophoresis applications
- Miniaturised transformers
- Complex and monolithic suspended structures in glass

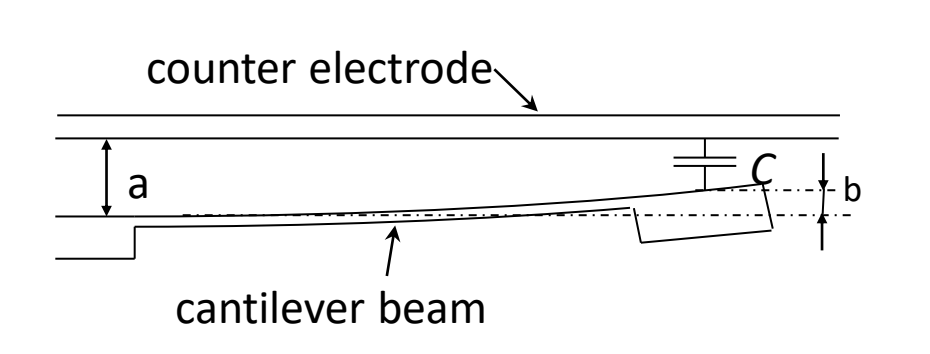


Glass accelerometer beam – capacitive read-out





- Mass = 4.87 mg
- Metallic backing plate
- Mechanical actuation
- Quality factor $Q = f_{res}/\Delta f = 100$ in air
- Deflection amplitude = $23 \mu m$ at 2856 Hz
- Acceleration amplitude : $A = 4\pi^2 b f_{res}^2 = 755g$



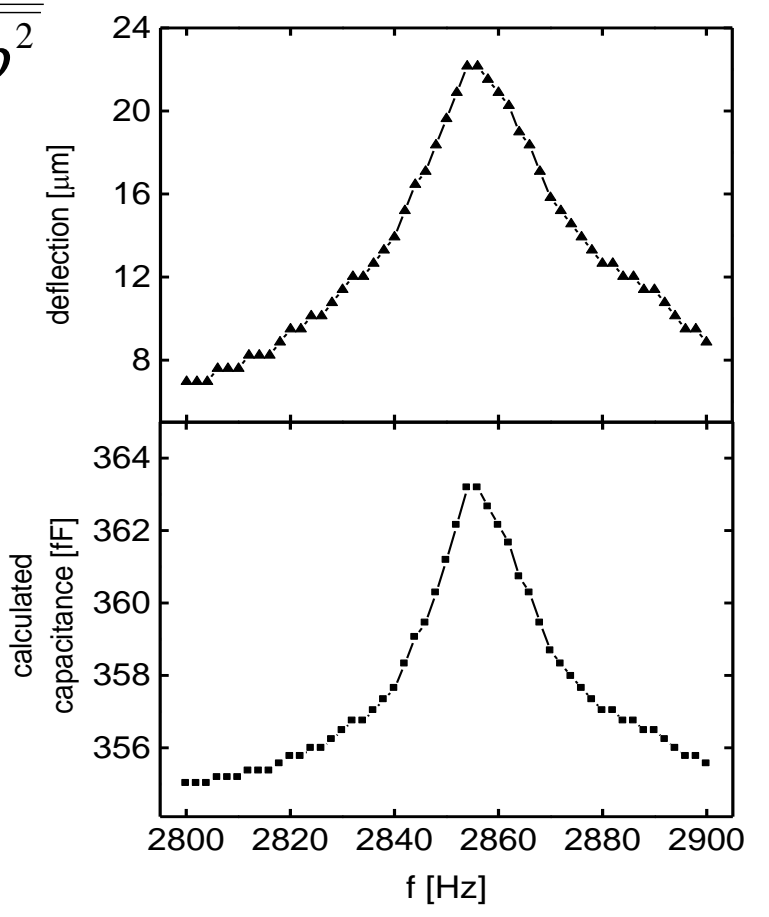
Calculated theoretical capacitance



$$C = \frac{1}{\pi} \int_{0}^{\pi} \frac{\varepsilon_{0} S}{a + b \cos \alpha} d\alpha = \frac{\varepsilon_{0} S}{\sqrt{a^{2} - b^{2}}}$$

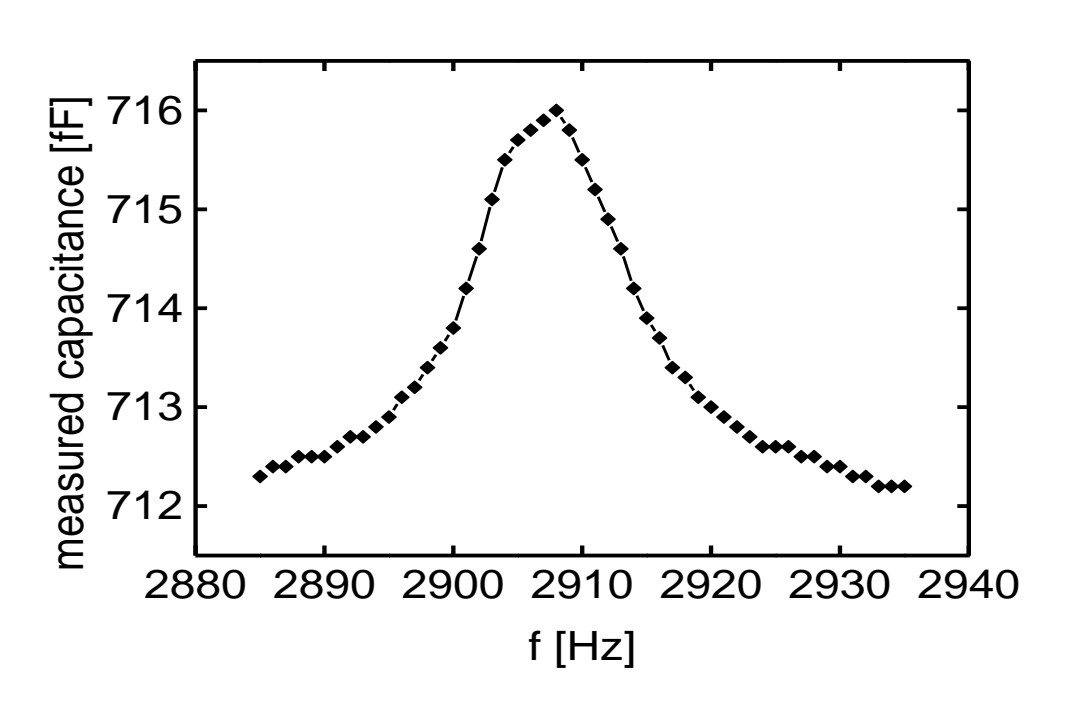
S: the capacitance surface

a: static gap



Measured capacitance



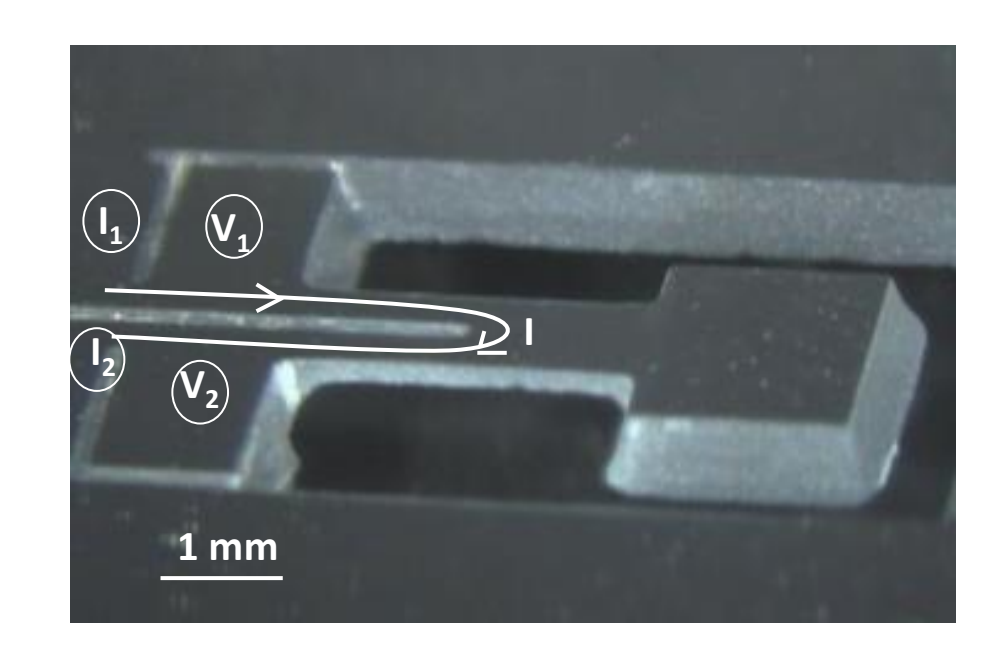


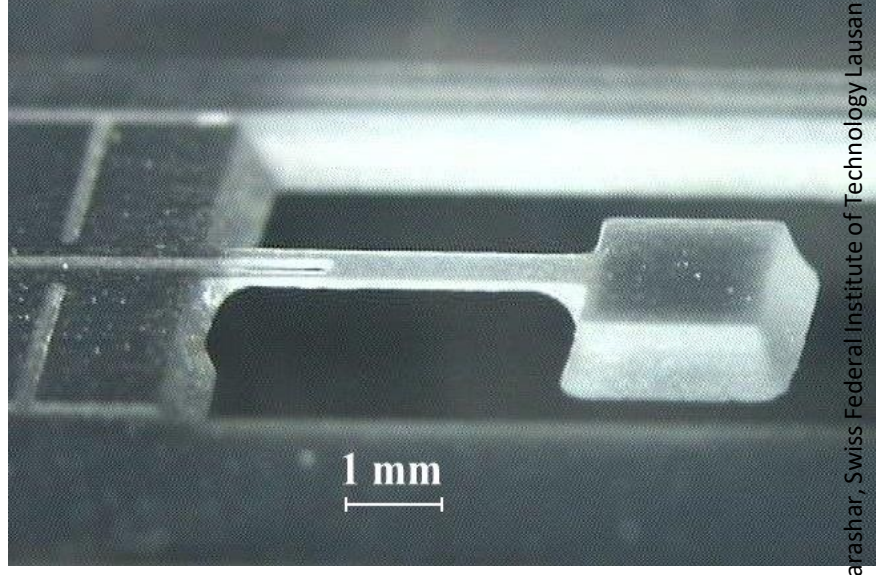
Capacitive sensitivity of 5.3 aF/g

anne (EPFL)

EPFL

Glass accelerometer beam – resistive read-out







$$\frac{\Delta R}{R} = \frac{\Delta l}{l} - \frac{\Delta s}{s} + \frac{\Delta \rho}{\rho}$$

$$\frac{\Delta s}{s} = -2v\frac{\Delta l}{l}$$

$$\frac{\Delta R}{R} = \left\{ (1 + 2v) + C(1 - 2v) \right\} \frac{\Delta l}{l} = K\frac{\Delta l}{l}$$

For Pt film : K = 2, with v = 0.3 and C = 1

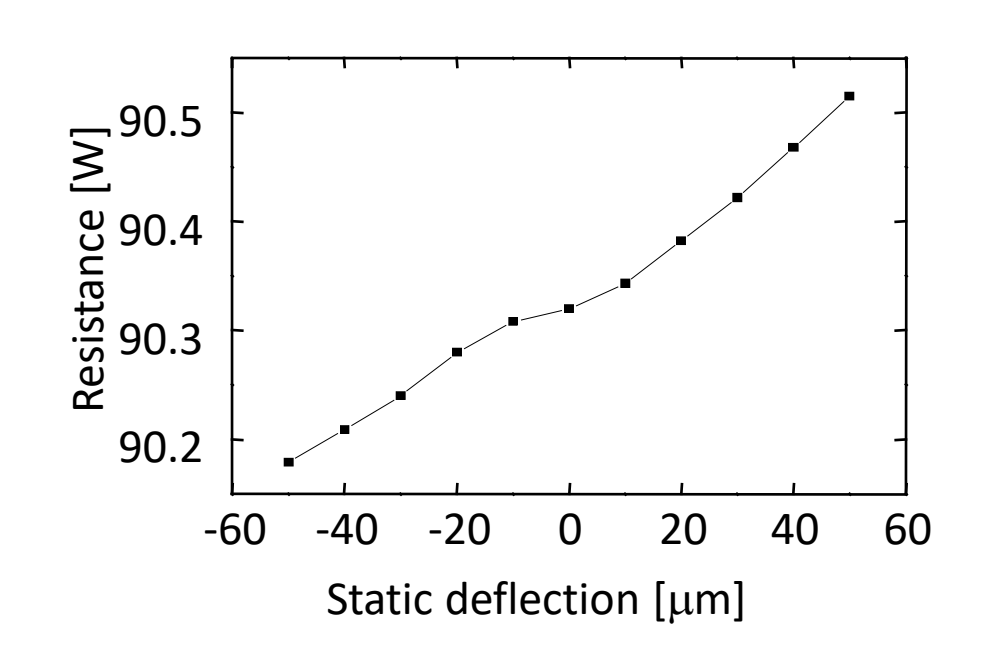
 \rightarrow

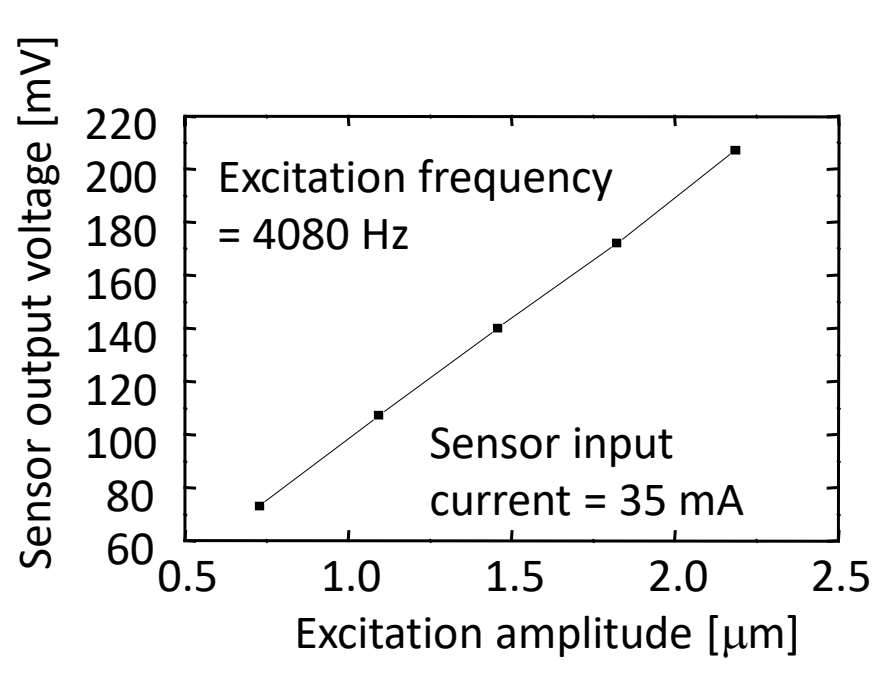
Macroscopic contribution is dominant

Prof. M.A.M. Gijs, Dr. V.K. Parashar, Swiss Federal Institute of Technology Lausanne (EPFL)

Glass accelerometers - resistive read-out

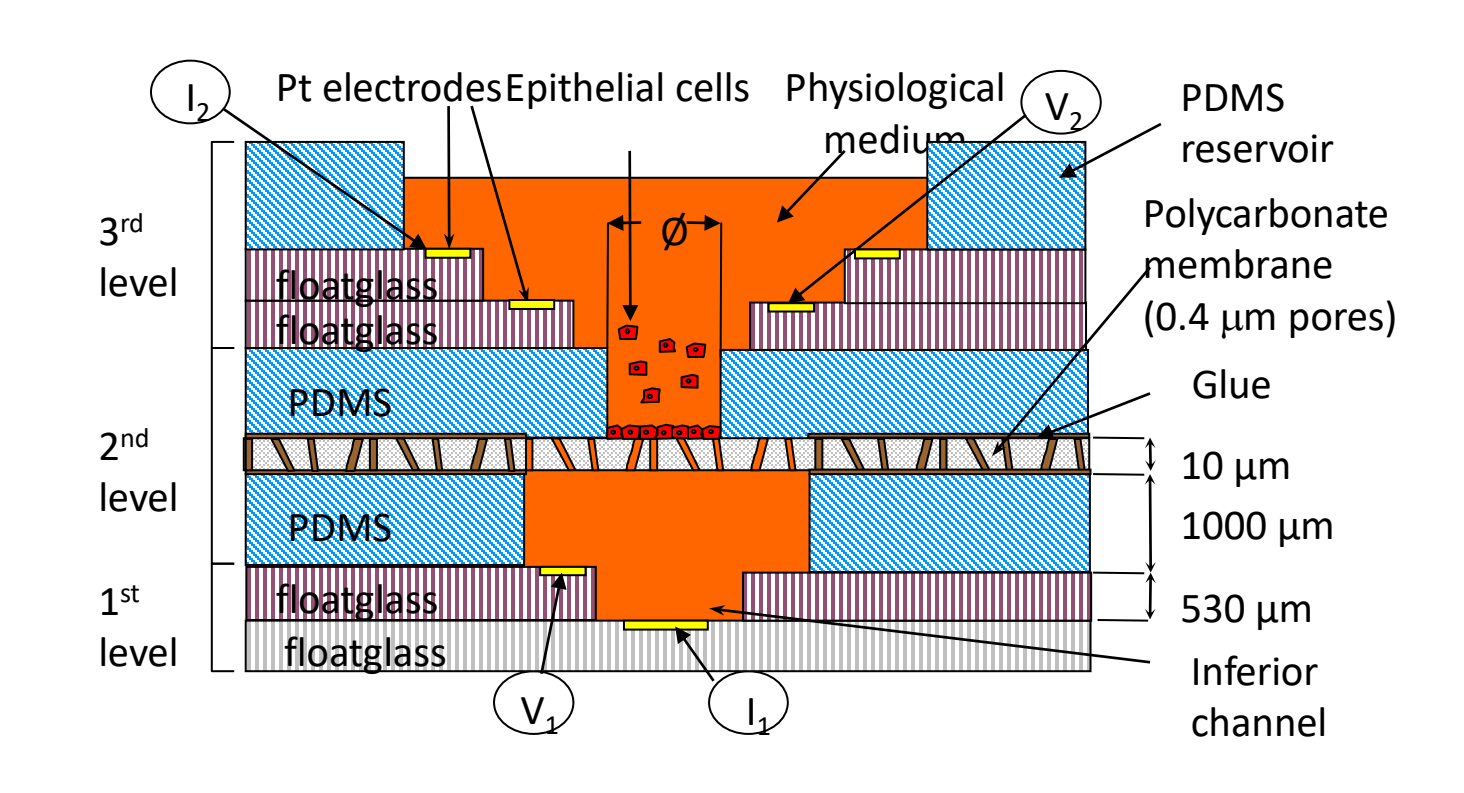






Miniaturised cell culture device

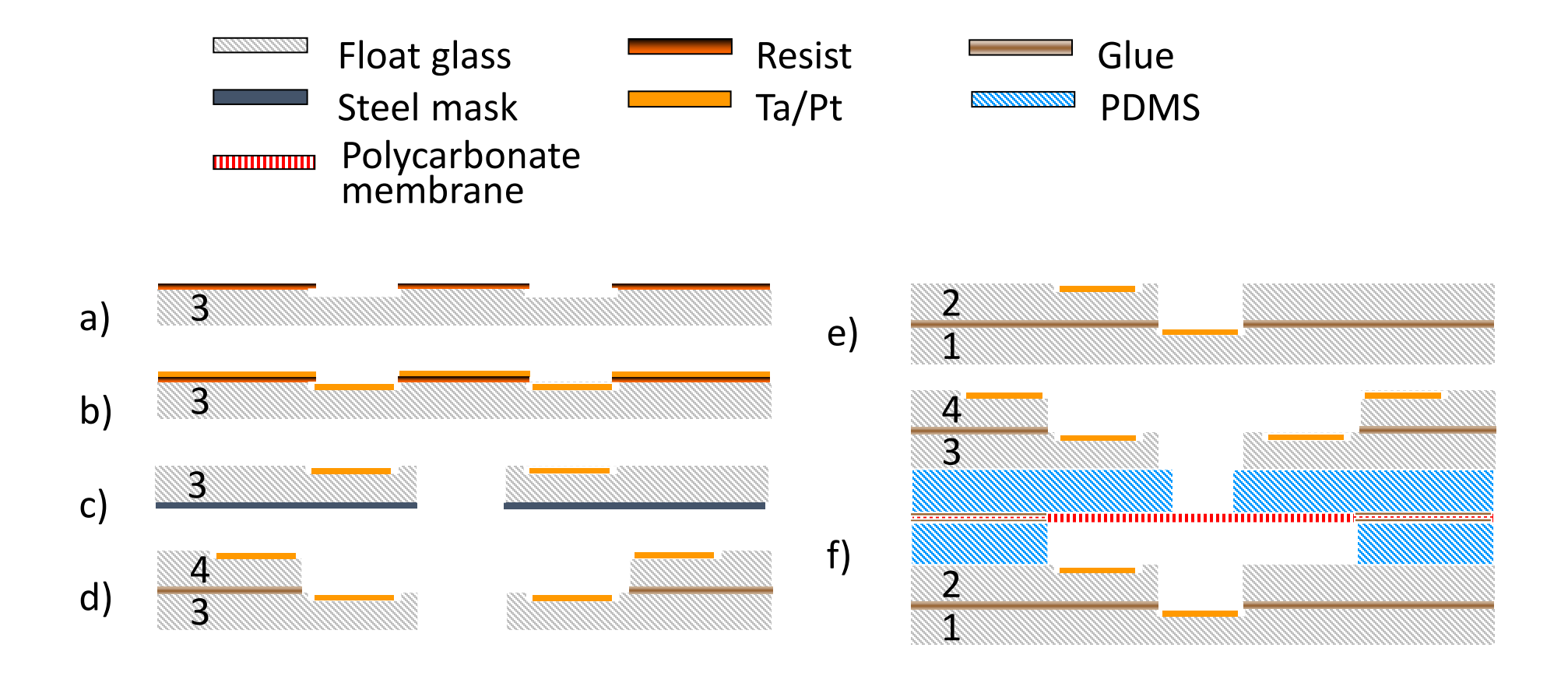




Prof. M.A.M. Gijs, Dr. V.K. Parashar, Swiss Federal Institute of Technology Lausanne (EPFL)

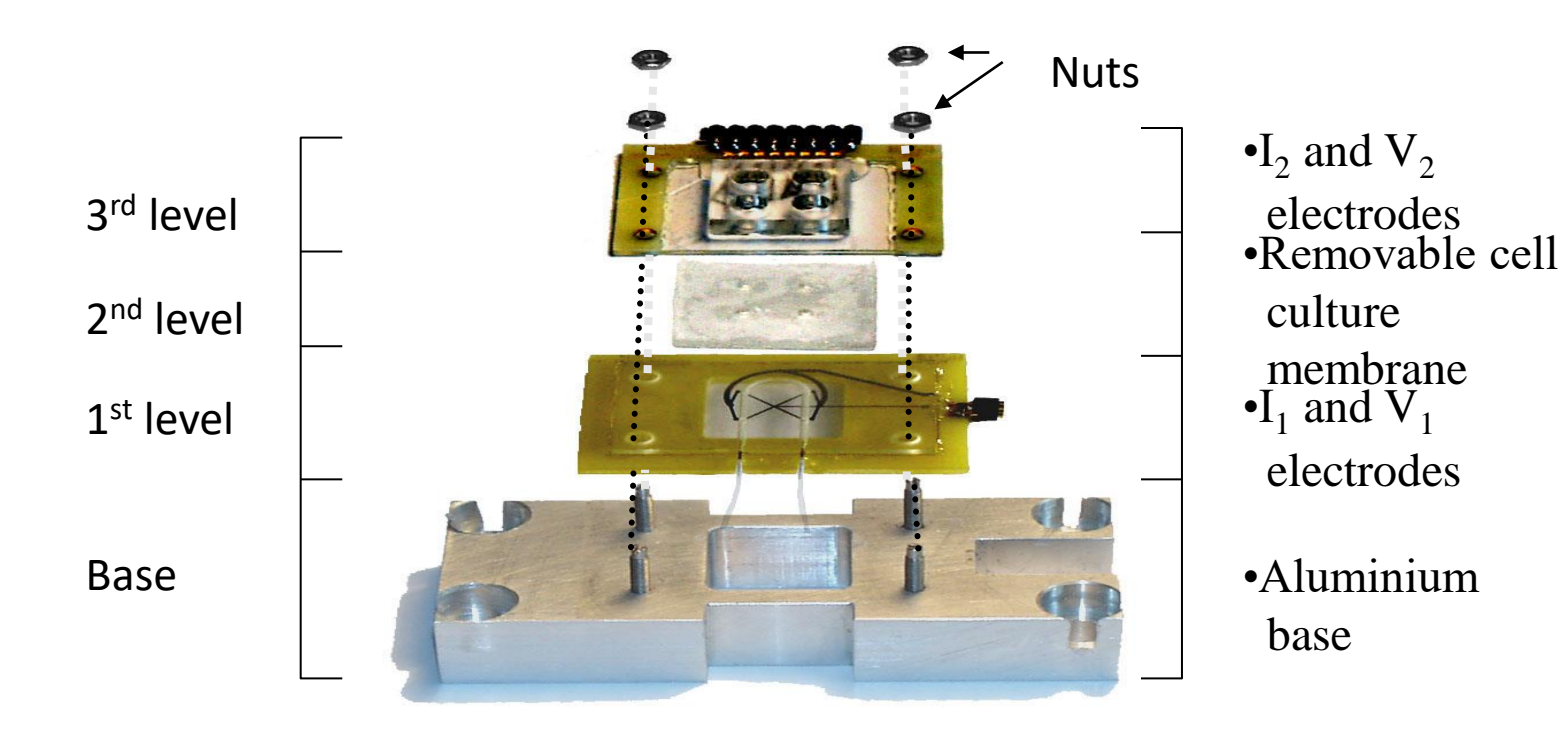
Cell culture device : fabrication



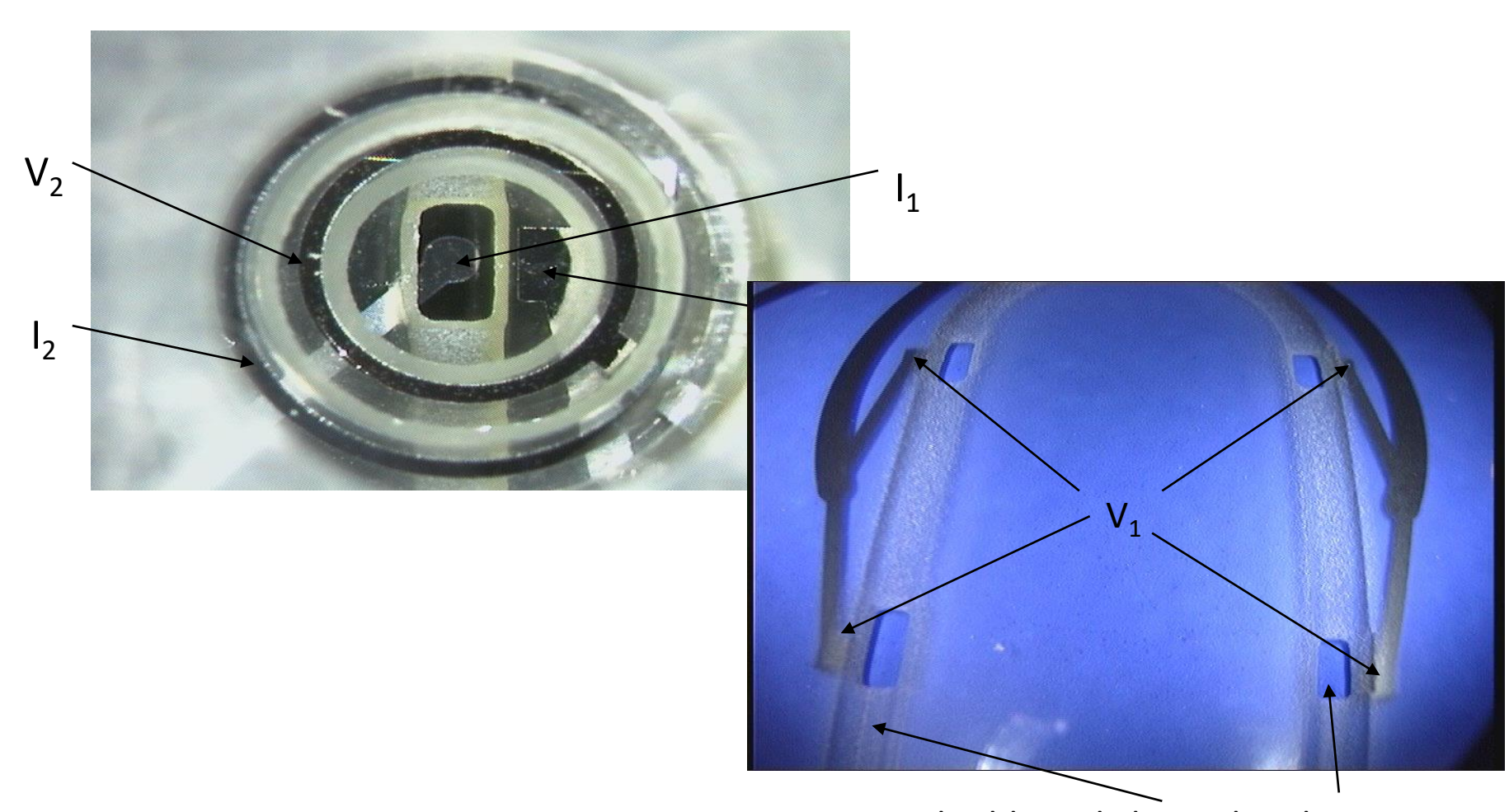


Modular cell culture device





EPFL

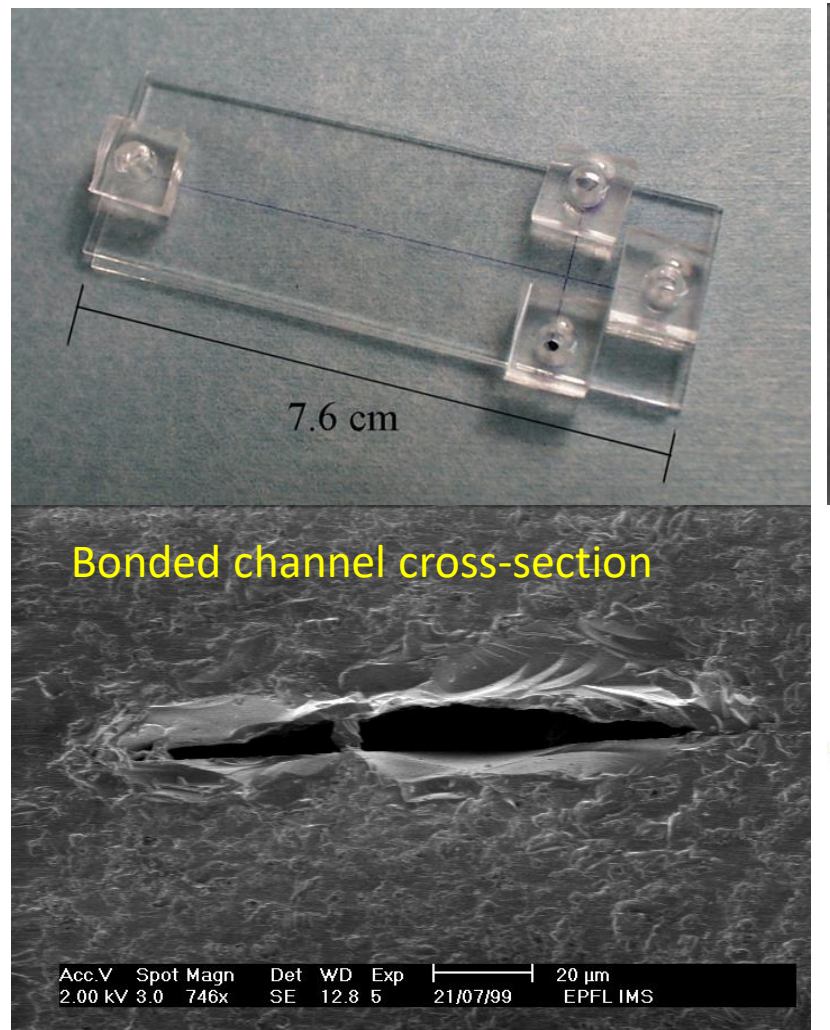


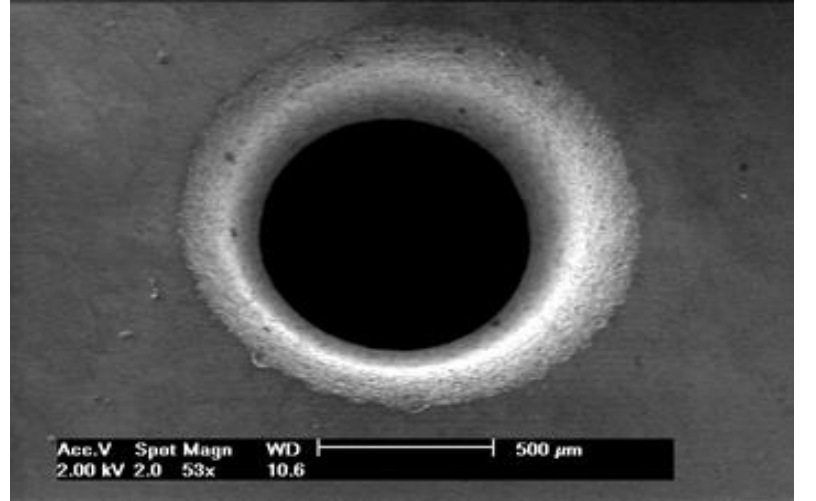
Powder blasted channel and vias

Prof. M.A.M. Gijs, Dr. V.K. Parashar, Swiss Federal Institute of Technology Lausanne (EPFL)

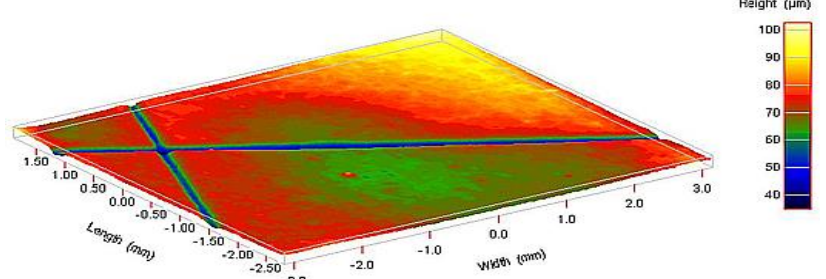
Capillary electrophoresis μ -chips







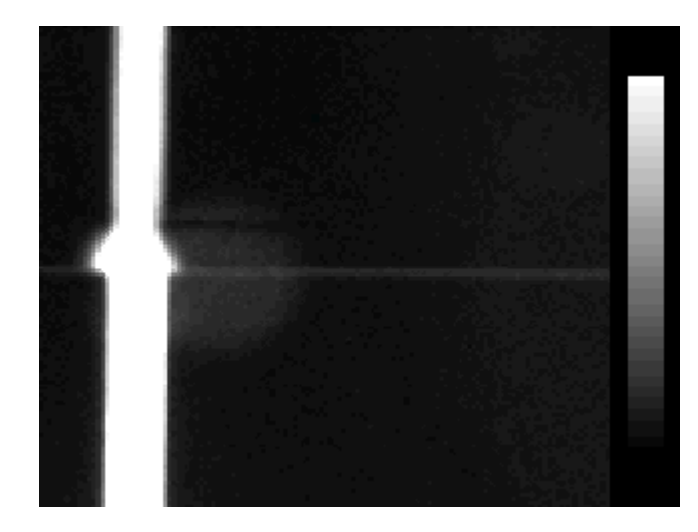
A. Sayah, D. Solignac, T. Cueni, M. Gijs, Sens. & Act. A 84, 103 (2000)



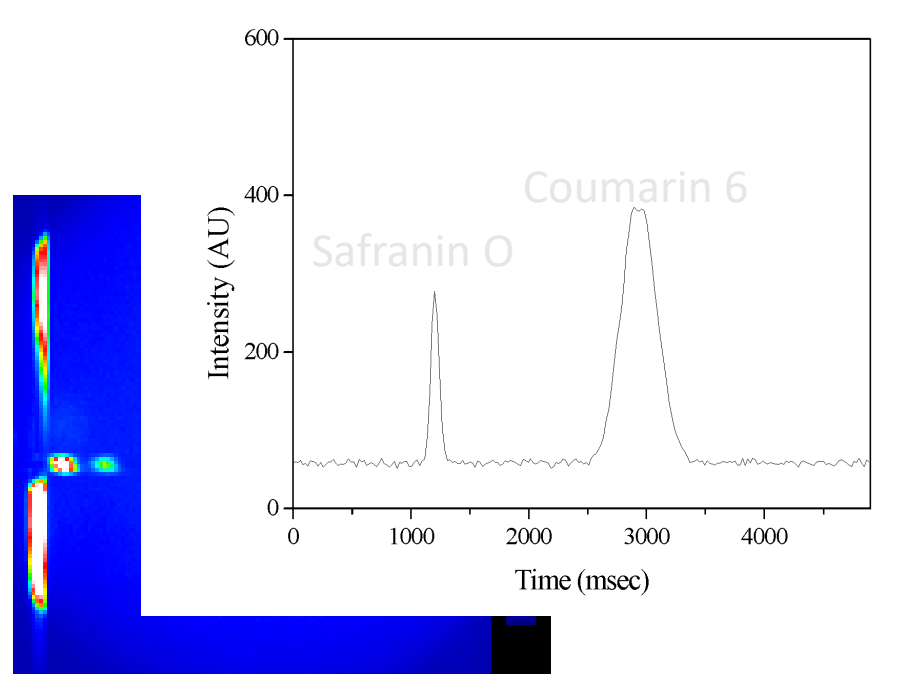
Capillary electrophoresis and electrochromatography

EPFL

Pinched electrokinetic injection Borate buffer (10 mM; pH=9.2) + fluorescein (20 μM)



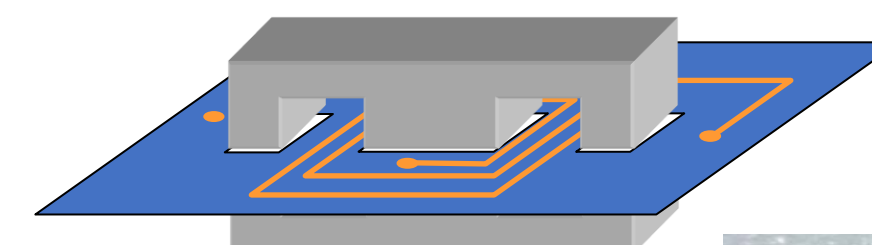
D. Solignac, A. Sayah, S. Constantin, R. Freitag, M. Gijs, Sens. & Act. A 92, 388 (2001) S. Constantin, R. Freitag, D. Solignac, A. Sayah, M. Gijs, Sens. & Act. B 78, 267 (2001)



Separation of fluorescent dyes coumarin 6 (30 μ M) and safranin O (30 μ M) in [ethanol 90% + borate buffer (10 mM) 10%]

Mini-transformers



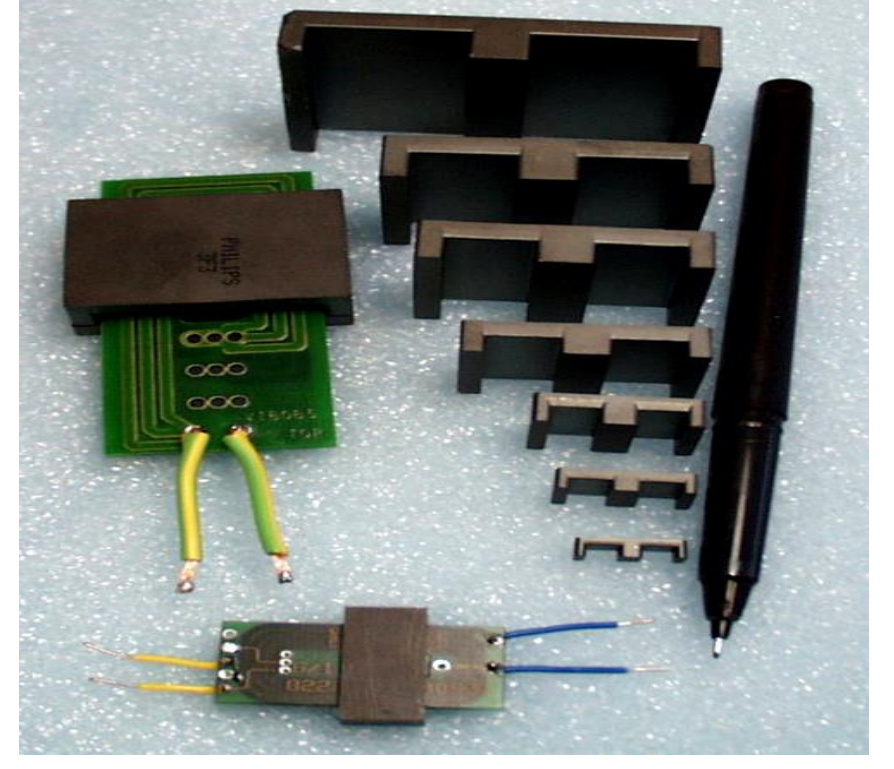


Combination of

E-shaped ferrite cores

with

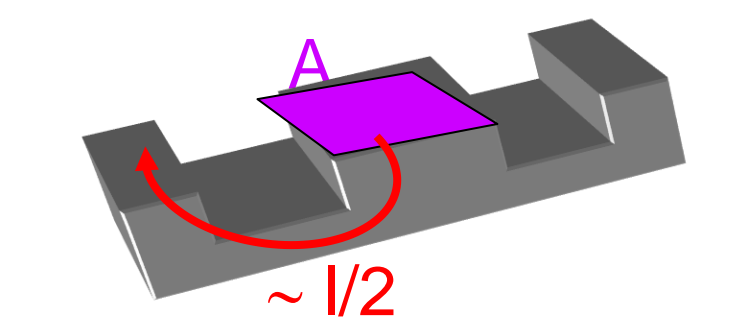
windings realised in Printed Circuit Board technology



Miniaturisation of inductive devices

'Simple' inductance formula:

$$L = \mu_0 \mu_r \frac{A}{l} N^2$$



Scaling down *A* and *l* with the same factor keeps *L* constant, but saturation of the magnetic core needs to be avoided

$$\Phi_{\mathrm{max}} = LI_{\mathrm{max}} = NAB_{\mathrm{max}}$$

with $B_{max} \sim 0.2$ Tesla

'Extreme' (mm) miniaturisation of inductive components

Applications

- Distributed, low power applications (0.1 1 Watt)
- Antennas
- Magnetic sensors

Issues

- Manufacturing of magnetic cores
- Handling and assembly

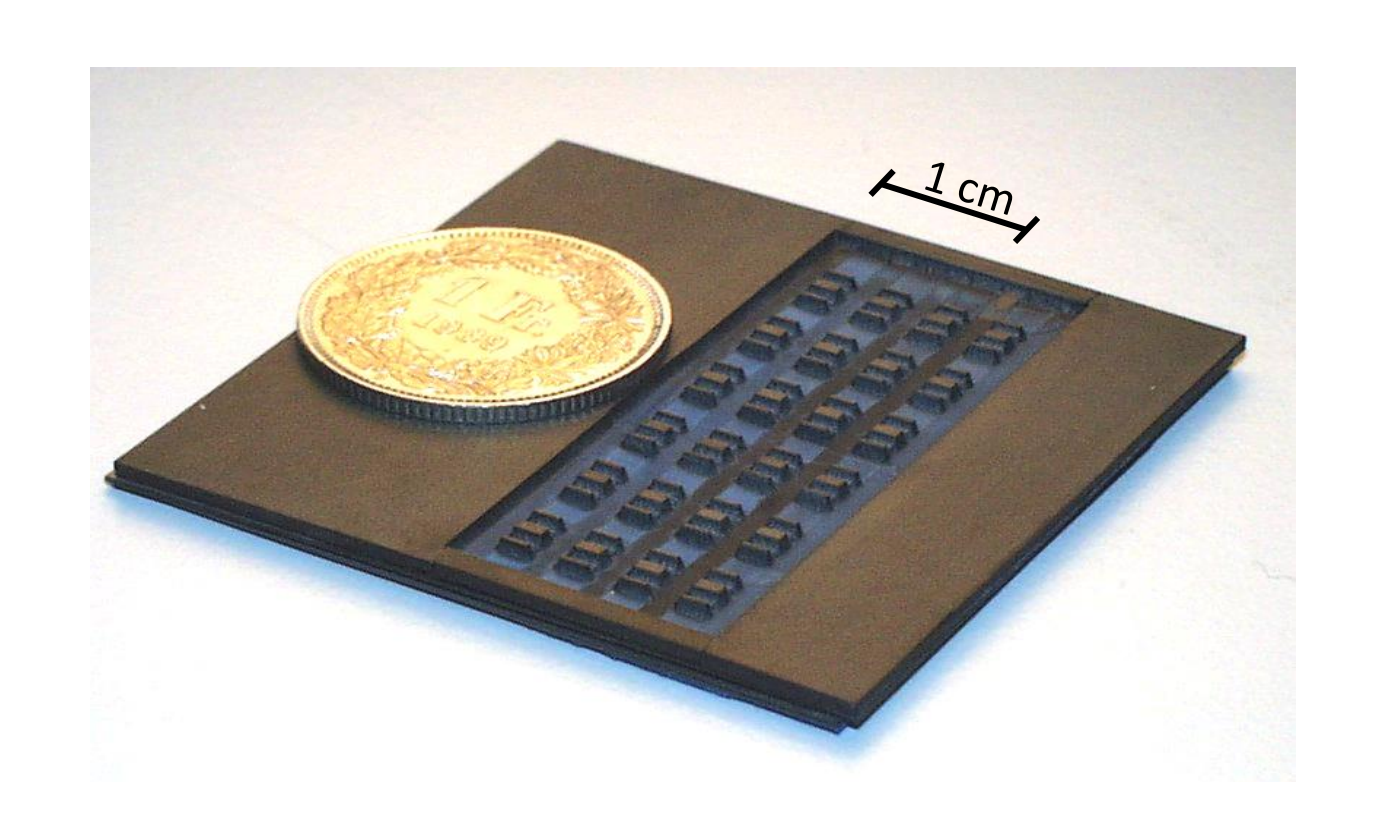
Our solution: batch-type technology

- Hybrid magnetic core PCB technology
- 3-dimensional microstructuring of ferrite wafers by powder blasting
- Wafer level handling and assembly of devices



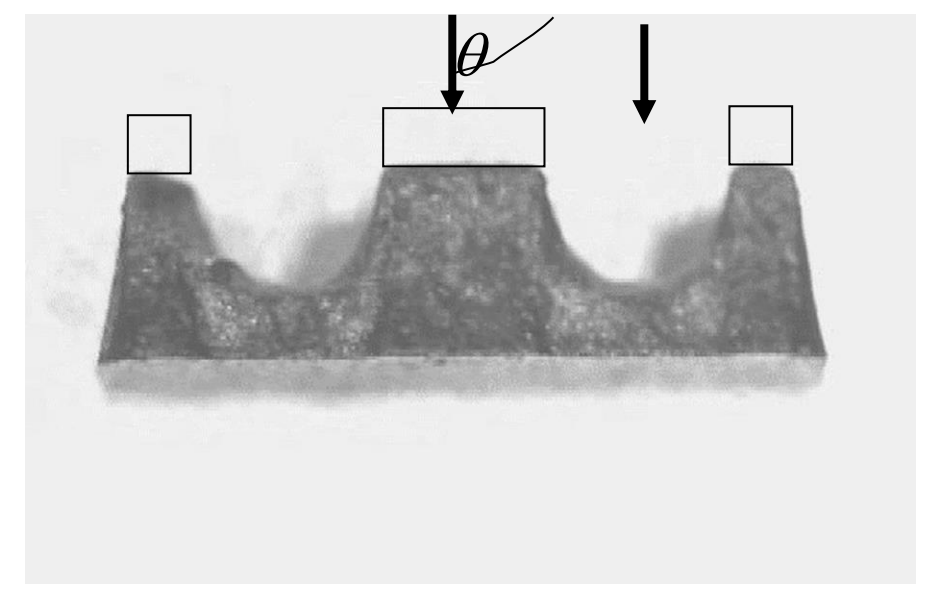
Powder blasting of ferrite wafers





'Natural' core profile





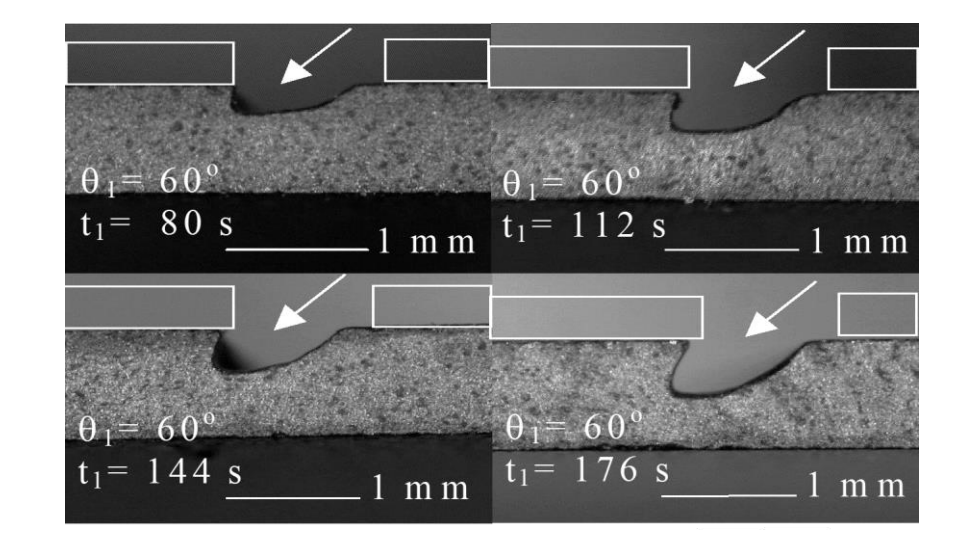
Powder jet at normal incidence (θ = 90°)

Profile is result of:

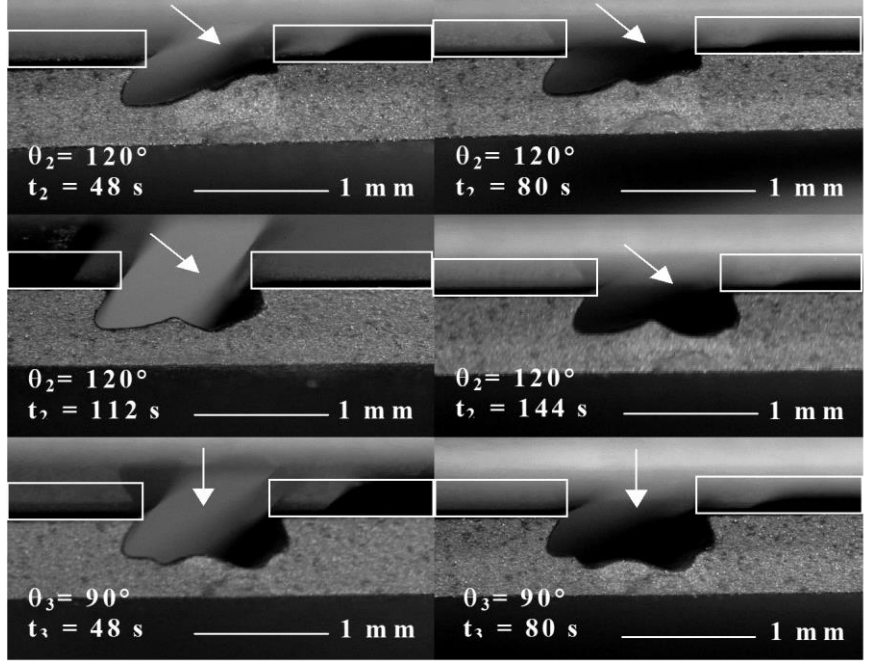
- particle finite-size effects
- angle-dependent erosion efficiency

'Tuning' the core profile



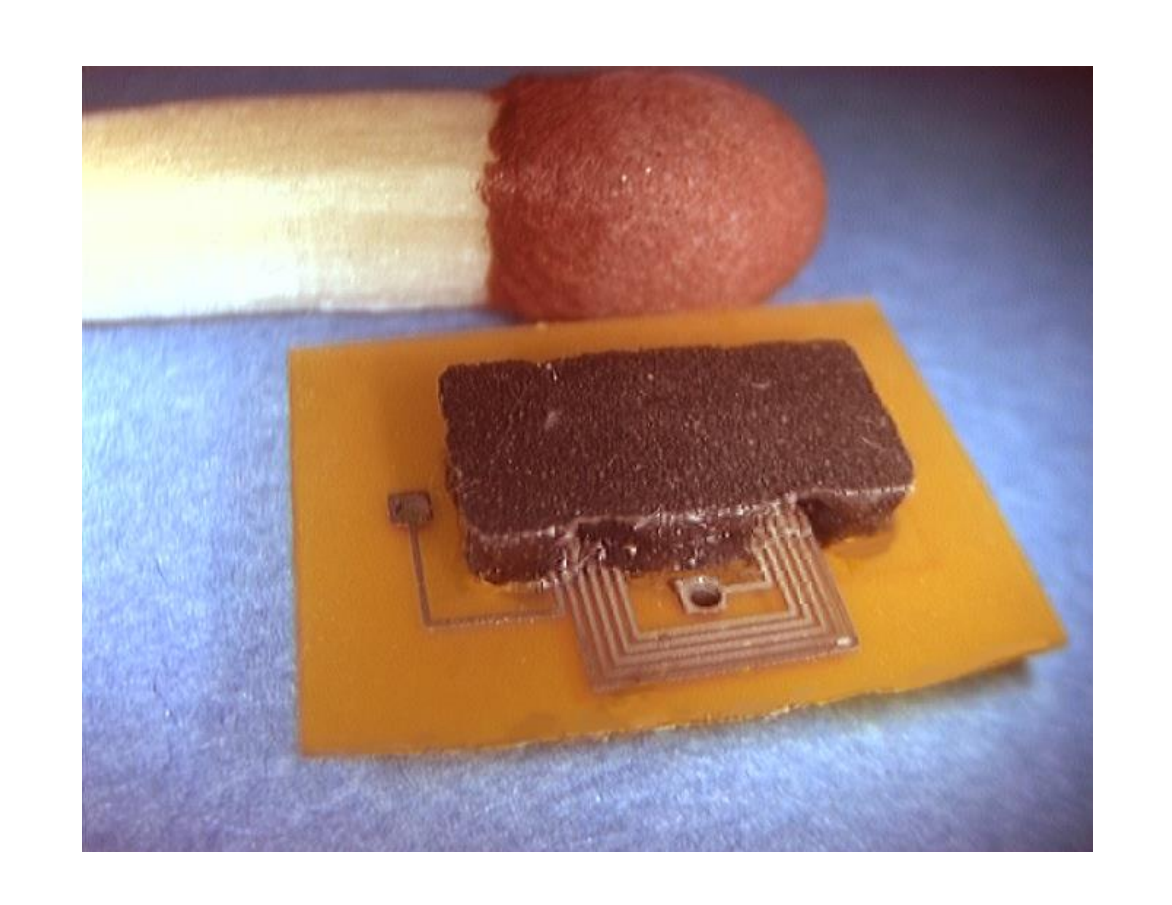


Powder jet at non-normal incidence



Assembled mini-transformer

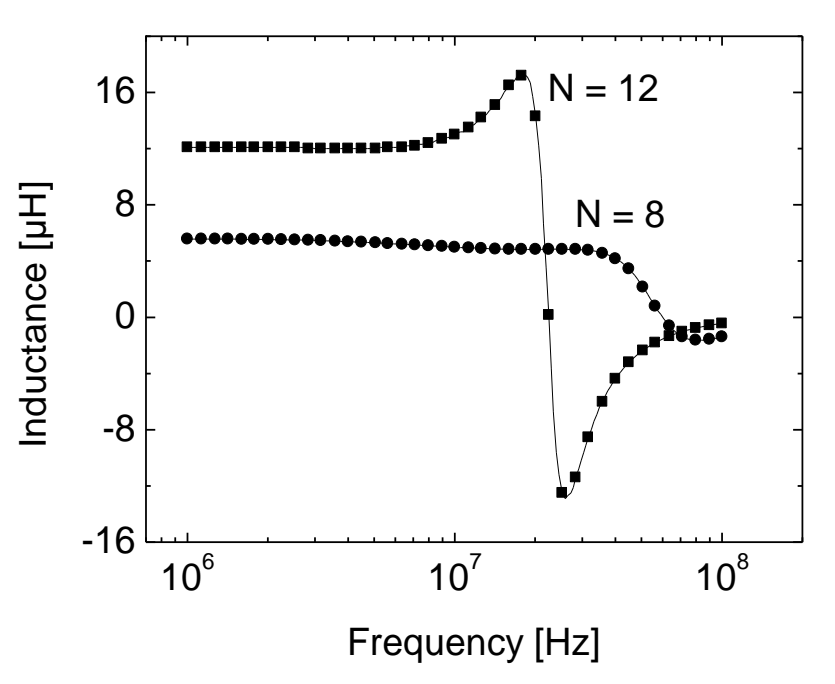


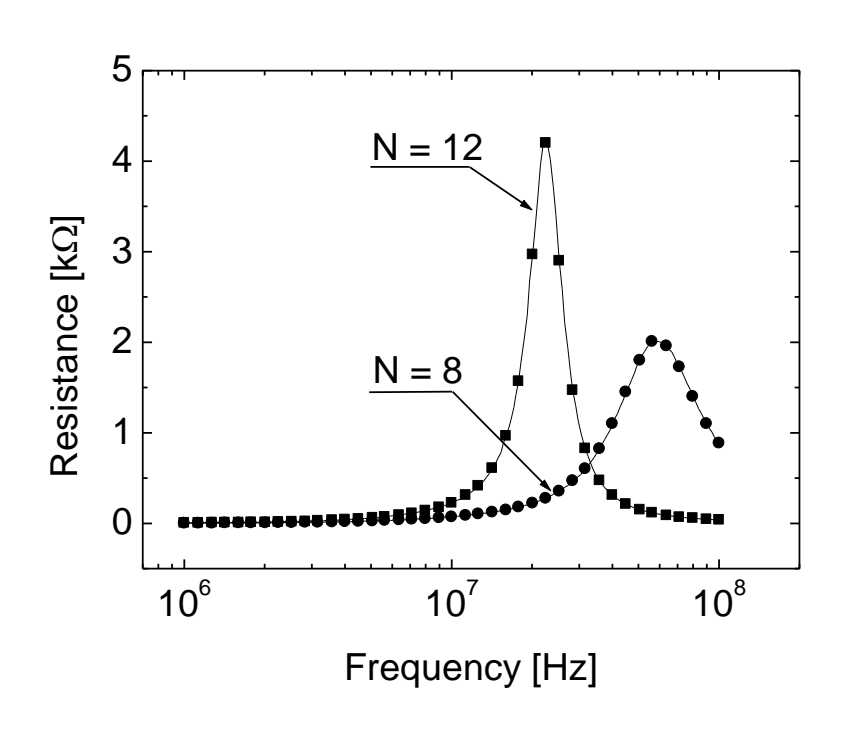


PEL) 2021

Inductance and resistance







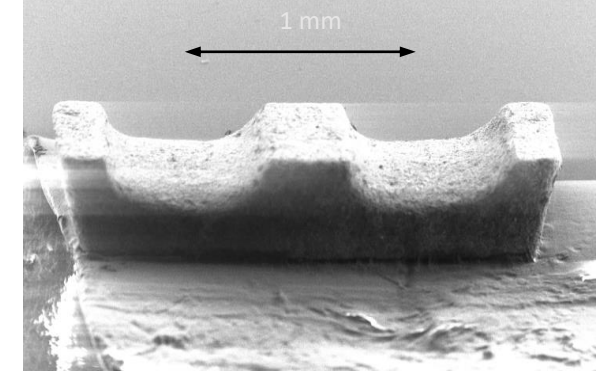
1,00

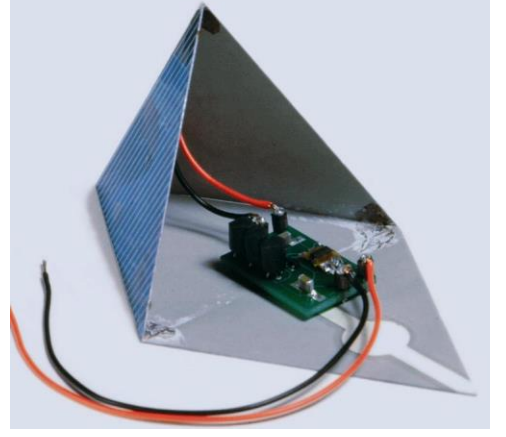
Prof. M.A.M. Gijs, Dr. V.K. Parashar, Swiss Federal Institute of Technology Lausanne (EPFL)

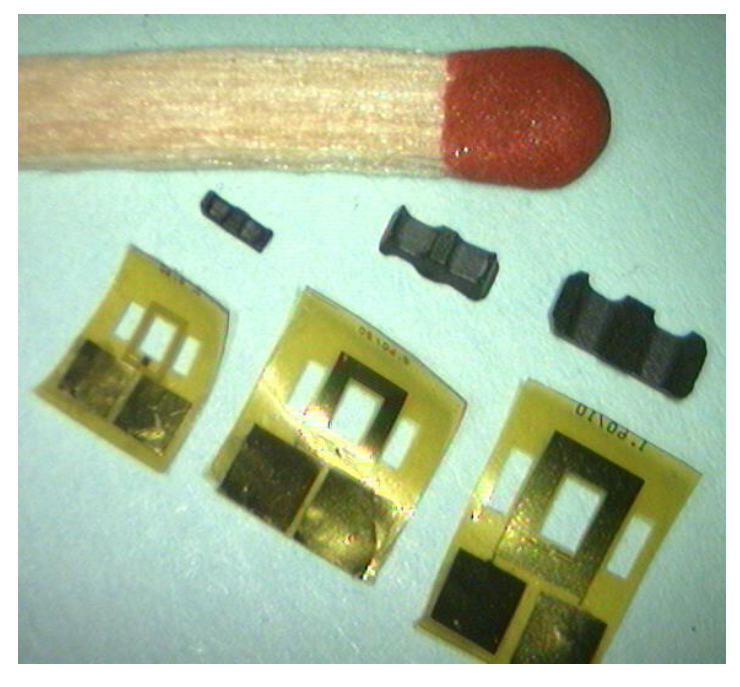
Representation of EPFL at the Hannover Messe 2002







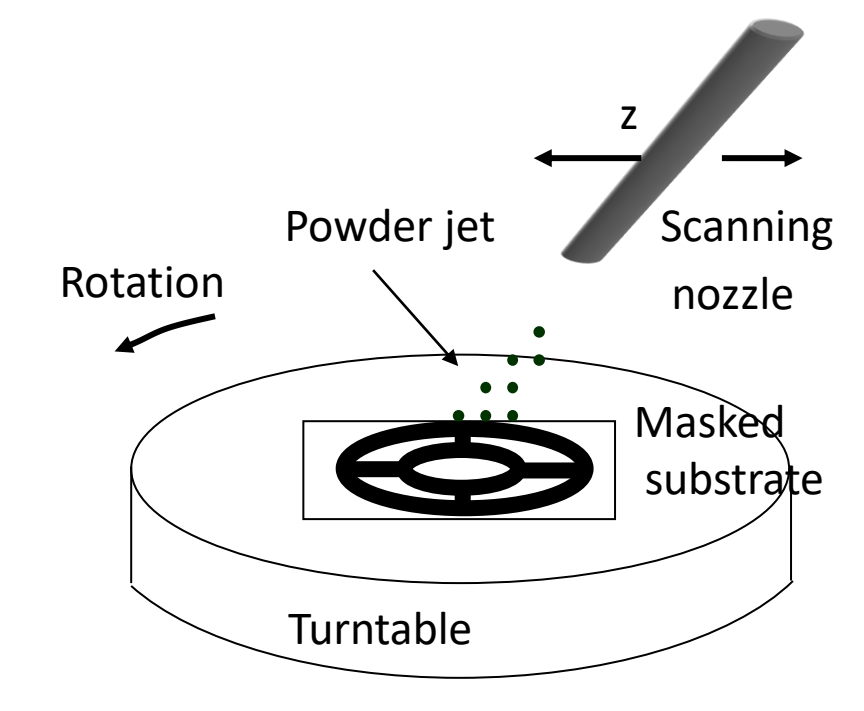






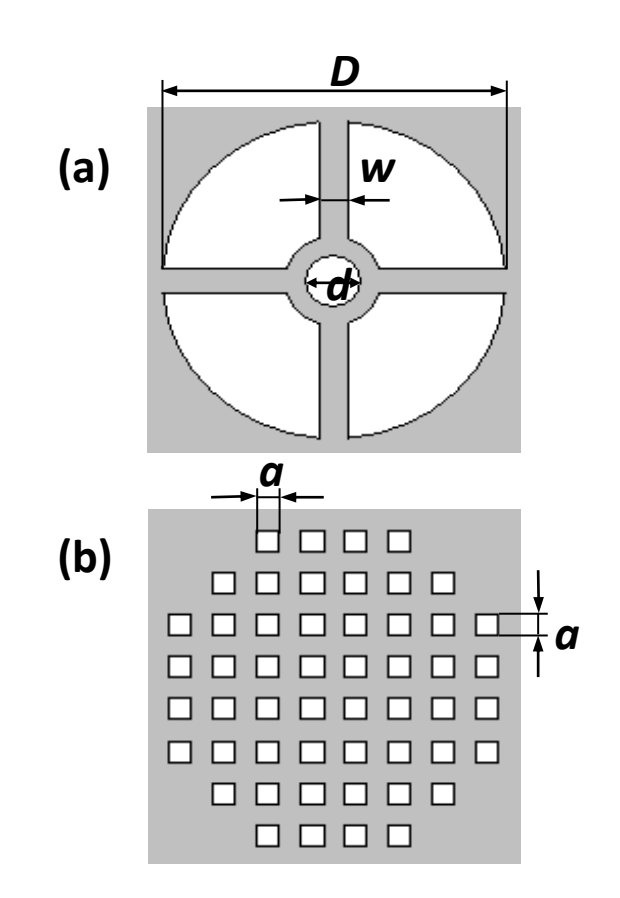
April 2002

Monolithic suspended structures in glass



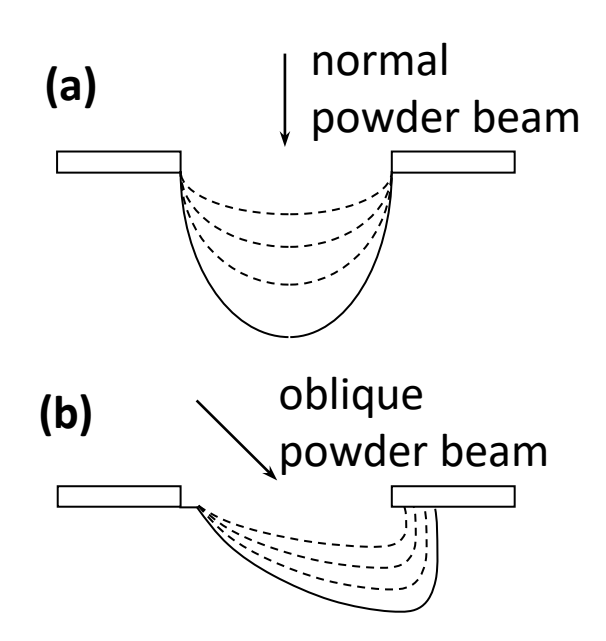
Experimental set up for the rotating mode of the powder blasting micro-erosion process



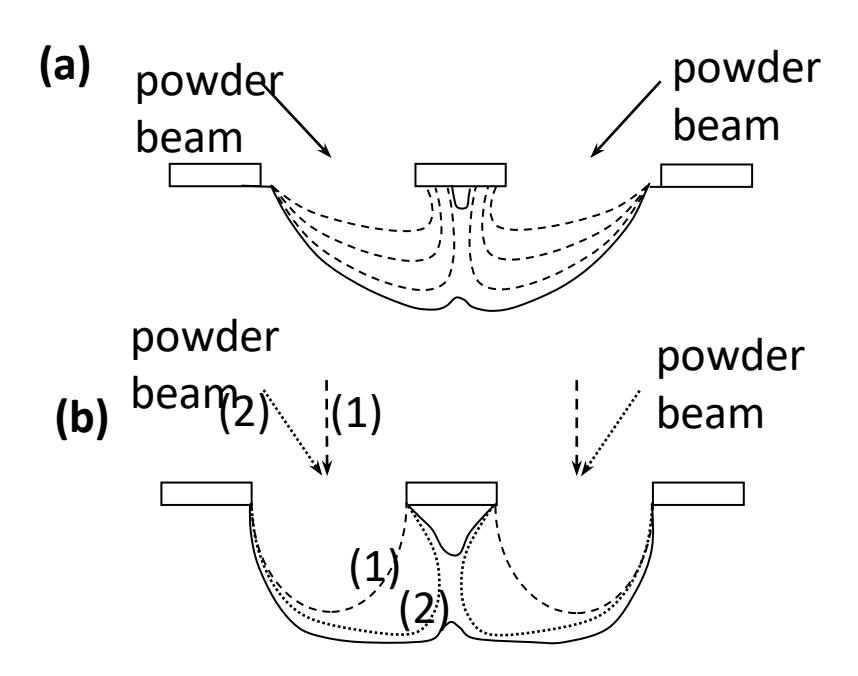


Mask sample design for the realization of (a) complex three-dimensional and (b) grid structures.





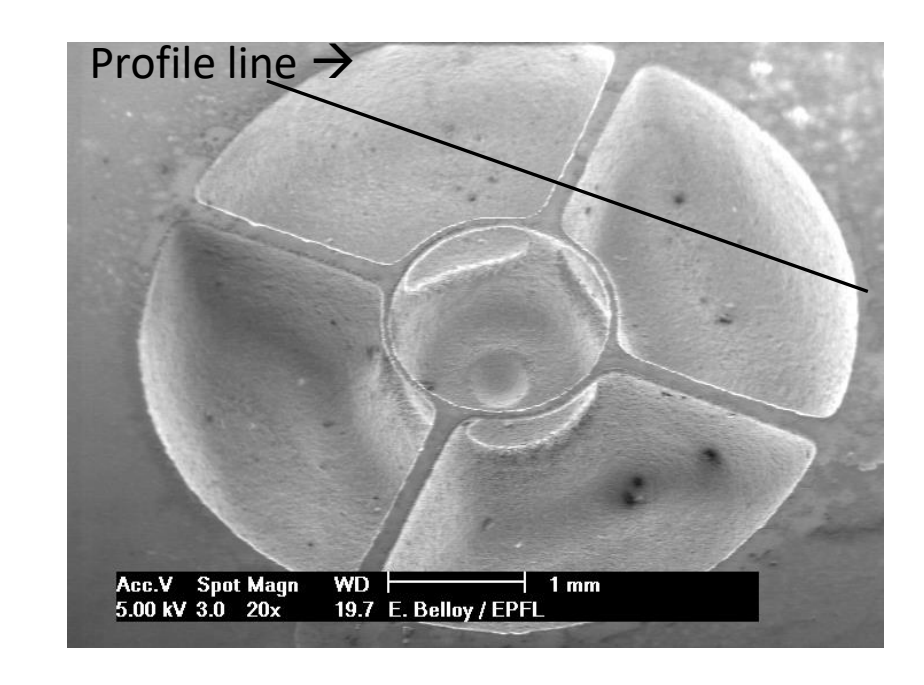
Schematic view of (a) a symmetrical hole obtained with a normal powder beam incidence and (b) a hole shape resulting of an oblique incidence of the eroding particles.



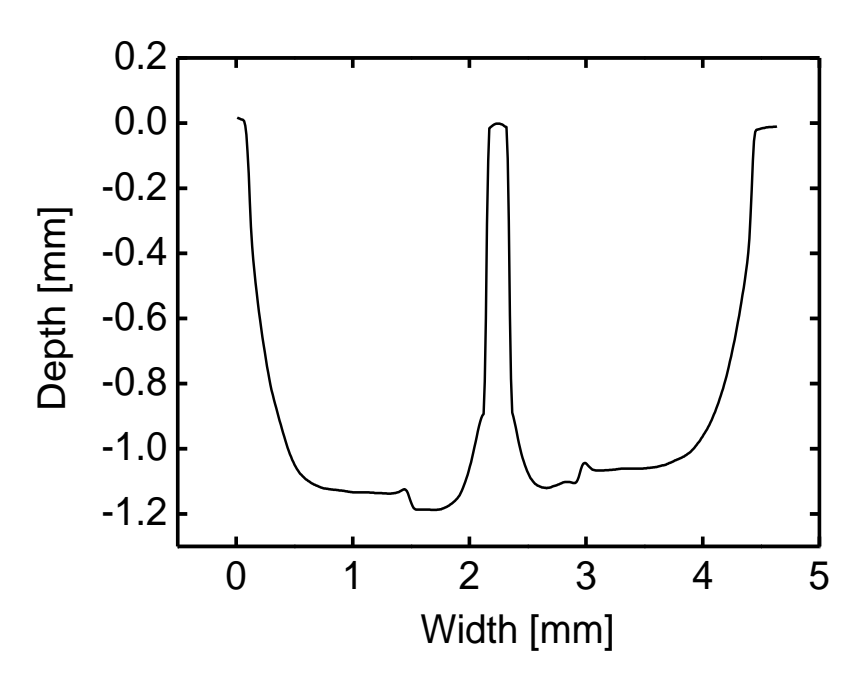
Schematic view of (a) suspended structure realised by one angle of incidence; (b) suspended structure obtained by alternatively using a normal and an oblique powder beam, which minimises the mask underetching effect.

High aspect ratio

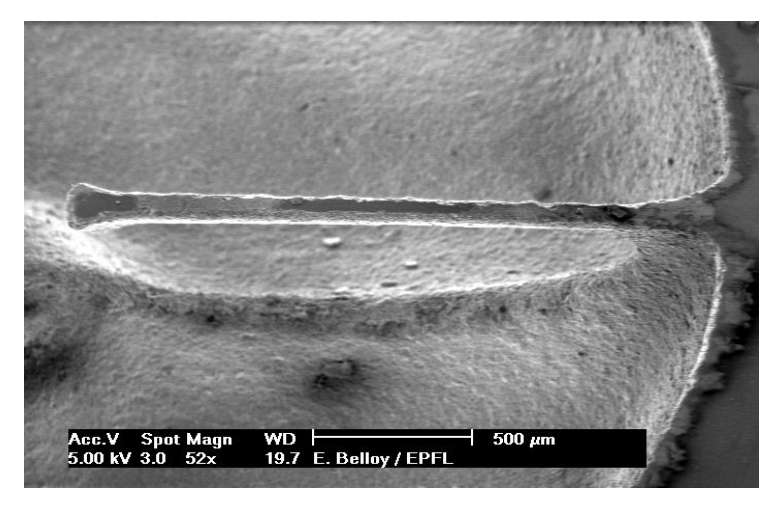




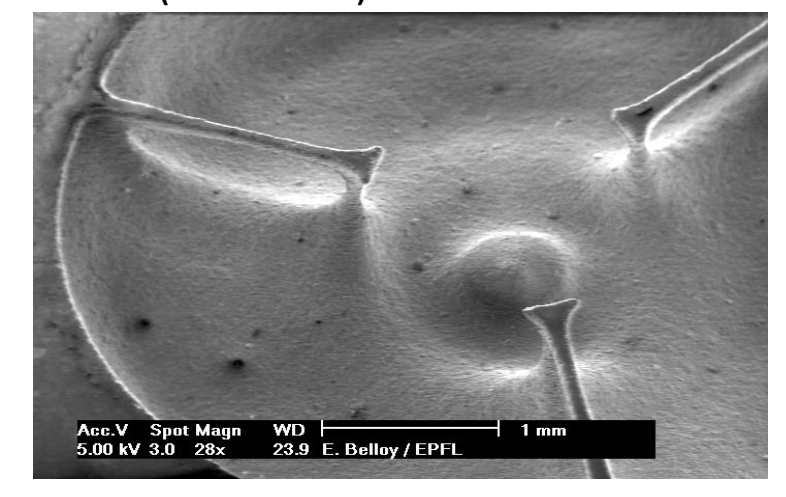
Scanning Electron Microscope (SEM) picture of a connected ring glass structure.



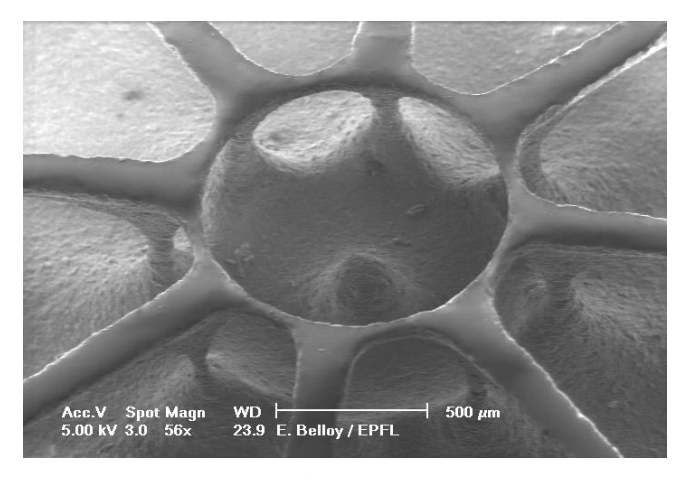
Profile of a high aspect ratio structure obtained using an optical profilometer. The structure width is 0.17 mm giving an aspect ratio of 7.



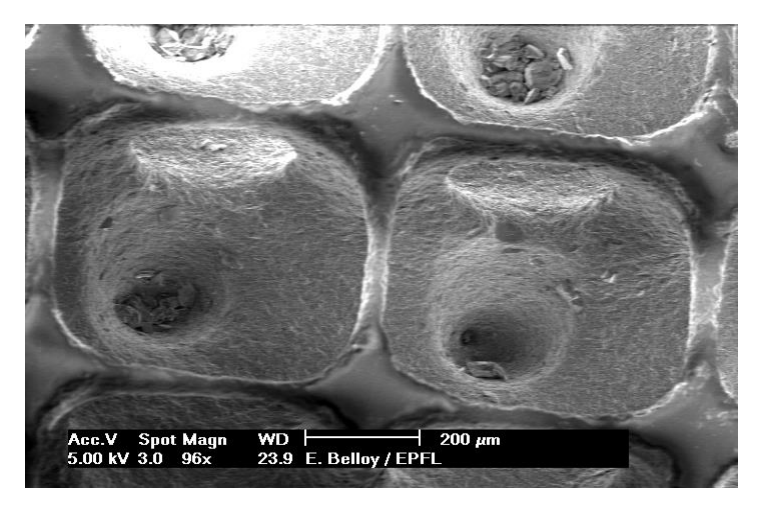
SEM picture of a 115 μm wide and 2 mm long suspended glass cantilever beam. (90° & 50°)



SEM picture of cantilever beams connected to the substrate on their extremity. (60°)



SEM picture of a complex threedimensional monolithic structure. (60° & 50°)



SEM picture of a monolithic grid structure. (90° & 60°)



References



- J.E. Shelby, Introduction to glass science and technology, The Royal Society of Chemistry, Cambridge, UK (1997)
- http://www.umist.ac.uk/MatSci/teaching/year3/ml352
- http://www2.cemr.wvu.edu/~imse304/raghav/raghav.htm
- P.J. Slikkerveer, Mechanical etching of glass by powder blasting, Ph.D. thesis Eindhoven University of Technology (1999)
- E. Belloy, A. Sayah, M. Gijs, Sens. & Act. A 86, 231 (2000); E. Belloy, S. Thurre, E. Walckiers, A. Sayah, M. Gijs, Sens. & Act. A 84, 330 (2000); E. Belloy, A. Sayah, M. Gijs, J. Microelectromechanical Syst. 11, 85 (2002)